NOTICE: When government or other drawings, specifications or other data are used for any purpose other than in connection with a definitely related government procurement operation, the U. S. Government thereby incurs no responsibility, nor any obligation whatsoever; and the fact that the Government may have formulated, furnished, or in any way supplied the said drawings, specifications, or other data is not to be regarded by implication or otherwise as in any manner licensing the holder or any other person or corporation, or conveying any rights or permission to manufacture, use or sell any patented invention that may in any way be related thereto.

ARPA ORDER NO. 347-62
PROJECT CODE NO. 7400

GENERAL MOTORS CORPORATION

TECHNICAL REPORT
ON

IONIZATION IN HYPERSONIC WAKES

REVIEW OF MICROWAVE PROBE INSTRUMENTATION AND SUMMARY OF PRELIMINARY DATA

HYPERVELOCITY RANGE RESEARCH PROGRAM
CONTRACT NO. DA-04-495-ORD-3567

DEFENSE RESEARCH LABORATORIES

SANTA BARBARA, CALIFORNIA

AEROSPACE OPERATIONS DEPARTMENT

TR62-209D

DECEMBER 1962

ARPA ORDER NO. 347-62
PROJECT CODE NO. 7400

Copy No 28

GENERAL MOTORS CORPORATION

TECHNICAL REPORT
ON

IONIZATION IN HYPERSONIC WAKES

REVIEW OF MICROWAVE PROBE INSTRUMENTATION AND SUMMARY OF PRELIMINARY DATA

PREPARED BY R. I. PRIMICH & R. A. HAYAMI

HYPERVELOCITY RANGE RESEARCH PROGRAM
CONTRACT NO. DA-04-495-ORD-3567

DEFENSE RESEARCH LABORATORIES
SANTA BARBARA, CALIFORNIA

AEROSPACE OPERATIONS DEPARTMENT

TR62-209D

DECEMBER 1962

TABLE OF CONTENTS

Section		Page
ABSTRACT		
PART I	REVIEW OF INSTRUMENTATION	1
I	INTRODUCTION	1
II	GENERAL REVIEW OF MICROWAVE PROBES	3
	Closed Cavities	3
	Free Space Techniques	5
	The Focused Antenna	9
	The Microwave Circuitry	10
	Theory of Interaction of Plane Waves with Plasmas	14
III	SUMMARY	20
PART II	APPLICATION OF FOCUSED PROBE INSTRUMENTATION TO FLOW FIELD STUDIES	21
	35 Gc, Four Beam, Amplitude Data	21
	70 Gc, Seven Beam, Amplitude Data	25
	35 Gc, Four Beam, Amplitude and Phase Data	28
	35 Gc and 70 Gc, Seven Beam, Amplitude and Phase Data	37
REFERENCES		62

LIST OF ILLUSTRATIONS

Figure	Title	Page
1	Attenuation of 35 Gc Beam by Hypersonic Wake	23
2	Attenuation of Four 35 Gc Beams by Hypersonic Wake	24
3	Location of Attenuation Peaks on Shadowgraph	24
4	Open Shutter Photograph of Hypersonic Wake	26
5	Image Converter Photograph of Model in Flight	27
6	Attenuation of 70 Gc Beam by Hypersonic Wake	29
7	Attenuation of Adjacent 70 Gc Beams by Hypersonic Wake	30
8	Attenuation of Adjacent 70 Gc Beams by Hypersonic Wake, Model with Angle of Attack	31
9	Radial Electron Density Gradients in Hypersonic Wake	33
10	Attenuation and Electron Density in Hypersonic Wake	34
11	Onset of Ionization Behind Copper-Capped Models	35
12	Electron Density Decay in Hypersonic Wakes Behind Copper-Capped Models	36
13	Ideal Disposition of Focused Beams in Hypersonic Wake	38
14a	Amplitude Attenuation in Seven-Beam, 70 Gc/ System	40
14b	Phase Change in Seven-Beam, 70Gc System	41
15a	Attenuation in Seven-Beam, 70 Gc System	42
15b	Phase Change in Seven-Beam, 70 Gc System	43
16a	Attenuation in Seven-Beam, 35 Gc System	44
16b	Phase Change in Seven-Beam, 35 Gc System	45

ABSTRACT*

In this report, an outline will be given of the progress which has been made in the development of the focused microwave probe as a plasma diagnostics tool, and in the application of it to the study of ionization in hypersonic wakes. Since a major part of the development has been concerned with instrumentation, the theoretical analysis of the interaction of the probe field with a plasma, data reduction, and interpretation of the results in terms of magnitudes and spatial variations of electron density and collision frequency, this report will deal with these topics in detail. Numerous results have been recorded and are now undergoing data reduction. These will be tabulated and samples will be given. Interpretation of these results in terms of their flowfield significance will be given in future reports.

*This research is part of Project DEFENDER, sponsored by the Advance Research Projects Agency, Department of Defense.

PART I
REVIEW OF INSTRUMENTATION

SECTION I. INTRODUCTION

A general review of microwave probe work will be given in this report. This review will not be comprehensive; instead, an attempt will be made to cover the various techniques in common use together with their main disadvantages. Consideration of these disadvantages led to the concept and application of the focused microwave probe. The theoretical and experimental evaluation of the focused field and its interaction with a localized plasma near the focus will be described. Special circuitry which had to be developed in order that the confined nature of the field could be exploited to measure electron density and collision frequency, will be discussed.

Emphasis will be placed on studies of the interaction of electromagnetic waves with various plasmas, since they are important in the reduction of probe data. In particular the underdense plasma approximation and its relation to the rigorous theory for uniform plasma slabs will be outlined. A numerical technique by which the scattering properties of a plasma slab, within which non-uniform ionization may exist, will be discussed. The relationship of these basic theories to the interpretation of the probe data in such a way that radial gradients in electron density and collision frequency may be deduced, will be dealt with in some detail.

The achievements in the development of the focused probe and its potential in flow field studies will be summarized.

Results obtained with the use of such probes in the General Motors Defense Research Laboratories Flight Physics Range will be tabulated. The status of the data reduction will be summarized. In general, all data has been reduced to the point where phase shift and attenuation per beam information is available. The program by which this information can be converted into magnitude and spatial variation of electron density and collision frequency is now being formulated. Samples of data, to the extent that the reduction has been completed, will be presented.

SECTION II. GENERAL REVIEW OF MICROWAVE PROBES

Ionization in hypersonic wakes has been studied with the aid of two general categories of microwave instrumentation, namely resonant cavities and free space probes.

CLOSED CAVITIES

The resonant cavity is usually a cylindrical metallic enclosure and, in this form, it is most suited to measurements made on a cylindrical plasma which is located along the axis. Under the right conditions, this technique can result in excellent sensitivity. For good operation, the diameter of the plasma should be small compared to both the wavelength and the cavity diameter. In addition the ends of the cavity should be closed in as much as possible. The results are difficult to interpret in the case that radial gradients of ionization exist, and, also, if axial gradients exist within the length of the cavity. In fact the spatial resolution is no better than the cavity length. The cavity technique has been discussed in some detail elsewhere[1 - 3].

In relation to hypersonic wakes, the technique has been thoroughly exploited at the Lincoln Laboratories[2]. With the use of frequencies as low as 450 Mc, electron densities as low at 10^{6-7} e/cc have been measured. In summary, it appears that the main drawbacks are due to the obstruction of the flow field, the limited spatial resolution and the difficulty of resolving radial ionization gradients.

The obstruction of the flow field by the small openings in the cavity end-plates appears to be a serious objection. The main interference will arise due to reflections of the bow shock off the edges of the opening and subsequent recompression onto the axis of the wake. If this recompression were sufficiently strong, significant perturbations of the wake ionization could result. There appears to be some evidence[4 & 5] that such reflections can cause measurable changes in wake ionization. It would certainly seem that definitive experiments ought to be carried out to establish whether the physical obstruction imposed by the cavity can produce measurable effects in terms of ionization changes or perhaps could cause a triggering of turbulence.

The spatial resolution, which is determined by the length of the cavity, can be a severe limitation, especially in the near wake. The desirability of having single-mode operation and using low-frequencies (for the measurement of low electron densities) appears to require an axial length of about 6 – 12 in. The use of microwave cavities (say in X-band) which would provide adequate resolution, would require cavities so small that the cavity walls might interfere with the wake itself. In addition the holes in the end walls would be so large that losses would be too high to make the device useful as a cavity.

If strong radial gradients of ionization exist in the wake, it is not possible to deduce their presence from the cavity measurements alone. Predictions have to be made, based on some assumed theoretical model, and then compared with the results. Since the best interpretation of cavity results requires that the wake diameter be very small compared with the wavelength it is not certain whether cavity measurements are sufficiently sensitive to discriminate various degrees of radial ionization gradients.

The above disadvantages do not rule out the successful application of cavities to ballistic ranges. To the contrary, they have in fact been used to obtain significant data concerning wake ionization. However these disadvantages do limit their utility and they have been a major factor in forcing investigations of other techniques.

FREE SPACE TECHNIQUES

Non-Focused Probes

This title is used to describe a system in which the wake is illuminated by a microwave antenna which is so located that the wake is in the far radiation field. If the latter condition is satisfied, even though the wake diameter may be some significant fraction of the beam size, it will be smaller than the beam and an appreciable amount of the incident energy will bypass the wake. This leakage energy can cause intolerable amounts of interference with the energy that passes directly through the wake. It is usual to measure the total forward scattered signal, since, in the ideal situation of plane wave incidence on an infinite, parallel-sided, plane, plasma slab, the interpretation of this signal in terms of the plasma properties is relatively straightforward. However in the situation described above, the results can only be correctly interpreted where they can be matched to predictions based on the case of incidence of a spherical wave upon an assumed cylindrical plasma with appropriate radial and axial ionization gradients.

If the back-scatter signal is measured instead, the diffraction errors due to the leakage may be avoided, provided that efficient use is made of absorbing material, but two other difficulties are still encountered. One is the difficulty of interpreting the results in terms of an assumed

model, as for the forward scatter signal, and the other is inherent in the back-scatter technique. In particular the measured absolute phase of the back-scatter signal includes a phase component which is due to the electrical length between some datum point and the point at which the reflection occurs. Since, in general, the reflected wave has a phase associated with it which is a function of the plasma properties and since the point of reflection is not known, it is impossible to interpret the measured phase in terms of the plasma properties. Relative phase variations as a function of time may be significant if the distance between the datum point and the point of reflection does not change, or alternatively, if the phase of the reflected wave does not change. These phase uncertainties do not arise in the case of the forward wave, since the reference length, which is the distance between the transmitter and receiver, remains constant.

Due to the physical nature of this type of system, adequate spatial resolution, which is determined by the antenna beamwidth, is a problem. Although it is usually better than for a cavity system, by virtue of the higher frequencies usually employed, it is always worse than the diameter of the wake. An immediate consequence is that the wake diameter cannot be deduced from the measurements. In addition the beam will illuminate a length of wake of the order of several wake diameters and any details in this length will not be resolved experimentally.

Despite these disadvantages, a non-focused probe has been widely used with varying degrees of success. Systems in X and K_A bands have been used at CARDE[6] and, within the resolution limits, useful data has been obtained on the growth and decay of ionized wakes behind projectiles. A far more intensive program has been pursued by the staff of the Lincoln Laboratories[2]. Extensive data has been

obtained on a large number of different types of projectiles over a wide range of conditions (see also Ref. 4)

Focused Probes

Most of the disadvantages of the closed cavity and non-focused probe can be overcome if a free space system is used in which the energy radiated from a microwave antenna is focused to produce a beam of the smallest possible physical dimensions, in the neighborhood of the ionized wake. Two main benefits derive from the use of such a system, if it is properly designed. First, the energy can be so well concentrated that a negligible part of it will bypass the wake. Consequently the transmitted signal may be treated, with excellent accuracy, as having all passed through the region of ionization. Secondly, in the immediate neighborhood of the focal plane, the constant phase contours are planes which are approximately parallel to the focal plane. Under these conditions the measured signal which is transmitted through the wake may be interpreted in a reasonably simple manner, since the interpretation can be based on the idealized situation of a uniform plane wave incident normally on a plane, parallel-sided plasma slab.

It is not always possible to design an efficient focused system for any given physical situation. The results will depend on the physical dimensions of the plasma and on the magnitude of the ionization properties. On one hand, wakes with small diameters have to be studied with wavelengths so short that diffraction errors can be ignored. On the other hand the corresponding microwave frequency has to be at least within two orders of magnitude of the plasma frequency in order that plasma effects may be measurable. However, projectile sizes in ballistic ranges

which are of practical interest are such that both of the previous requirements are compatable.

Although focused antennas have been used for a number of purposes, very little success has been reported in their application to plasma diagnostics. The first known application is the Naval Research Laboratories work in which a focused beam was used to probe the ionized wake of rocket exhausts[7]. A great deal of the development work has been reported, but it is not known (to the author) what degree of success has been attained. From the known information it appears that the focused system was not used in the most efficient way. In particular the "depth of focus" appeared to be small compared to the diameter of the plasma, which would mean that the effective width of the beam would be much greater than in the focal plane. In addition strong radial gradients which probably exist would not be revealed, especially since no more than one beam appears to have been used. It is believed that focused microwave systems have been used at the Applied Physics Laboratories of John Hopkins University, although no reference to this work is known to the author. One beam focused probes have been installed on the AVCO ballistic range, but no results were reported[3]. More recently, interest in the focused probe has been shown among workers in the thermo-nuclear fusion field. Extensive use of focused systems has been proposed[8] at millimeter wavelengths, but no results have yet been reported. Investigations are now underway at Princeton[9] on focused systems and it has been indicated[9] that large errors have been observed in the results obtained with the use of non-focused beams.

The present work on focused probes has been a continuous effort, which started at the Defence Research Telecommunications Establishment,

Ottawa, Canada, in 1956. Much of the early effort was devoted to detailed studies of the field distribution near the focus, resolution properties and transmission through a focused system (Ref. 6) Although a great deal of theoretical and experimental work on focused antennas had been available the above investigations were needed since none of the publications covered apertures of unity focal ratio which were adopted because of their maximum resolution possibilities. This work culminated in a four-beam system which was placed in operation on one of the ballistic ranges at the Canadian Armament Research and Development Establishment, in Canada (Ref. 10), The circuitry of this first probe was not sufficiently sophisticated to enable unambiguous interpretation of the data to be made. However if the wake were sufficiently underdense, the probe data could be analysed and appeared to be excellent.

Further discussions of the probe development will be simplified, by breaking them down under the three headings to follow, which categorize the three major problem areas.

THE FOCUSED ANTENNA

The properties of the particular focused antennas which have been used at both DRTE and DRL have been described in some detail (Refs. 6 and 11) and it is worth recalling only the main features here.

Focused apertures, with focal ratios of unity, have virtually yielded theoretical performance in terms of spatial resolution. In practice this means that most of the beam energy can be transmitted through a circular area, the diameter of which is about two wavelengths in the focal plane. Alternatively two identical targets, which are located in the

focal plane may be resolved provided that they are spaced one and a half to two wavelengths apart.

A theoretical analysis of the power flow between two focused apertures was carried out for the purpose of estimating the amount of power which could be channeled through circular areas of finite size located in the focal plane. (Ref. 12) It is evident from the latter results, if interference effects which arise from energy leaking around the wake are to be kept within, say, three decibels, then focused beams have to be used and the illumination over the radiating aperture has to be quite strongly tapered.

It has been found that good focusing is maintained where the antenna feed horns are moved as much as one inch off axis. This property has been used to provide a system of several independent beams through one lens system. In particular a vertical array of adjacent beams has been used to form a fence across the flight path in order to ensure interception of the ionized wake and also to provide information on radial variations of ionization. The CARDE system (Ref. 10), which is believed to be still in use, has four 35 Gc beams. Each beam is approximately one half inch in diameter and the four beams cover a two inch strip in the direction normal to the flight axis. Two systems are currently in use at DRL, one, a 35 Gc system, which has seven staggered half inch beams, spaced one quarter inch apart in the vertical direction; the other, a 70 Gc system, which has seven, adjacent, quarter-inch beams, spaced a quarter-inch apart in the vertical direction. (Ref. 11)

THE MICROWAVE CIRCUITRY

The problems to be considered here are independent of the nature of the antenna field and are directly concerned with the type of circuitry that should be used to measure the desired signal parameters.

A great deal of the early plasma work was incomplete in that the measured data could not be resolved into the ionization parameters (electron density and collision frequency), without making many unjustified assumptions. For instance many measurements have and are being interpreted based on a paper by Whitmer(Ref. 13), in which it was shown that the average electron density can be derived from the measured phase of the transmitted signal and that the collision frequency can be obtained from a measurement of the attenuation, provided that the plasma is extremely underdense. (Ref. 11) It is also necessary to assume that the dimensions of the plasma are known and that the ionization is uniform. These assumptions are not always valid. However it has been shown that the underdense approximation has a much wider range of validity and, under these conditions, the plasma parameters may be derived from a measurement of the magnitude and phase of the transmitted wave. Consequently in future discussions it will be assumed that a microwave circuit, to be acceptable for use as a plasma probe, must at least have provisions for the measurement of both amplitude and a phase of the transmitted signal.

In reality any circuit which can be used to measure both the amplitude and phase, could be considered for plasma studies. Provision has to be made for the fact that in ballistics range work, fast transient measurement and recording of the signals is required.

One of the first circuits which appeared to be suitable for the present purpose, was used at Stanford University to obtain the magnitude and phase of the signal back-scattered by meteor trails. This was done by measuring the in-phase and quadrature-phase components of the input signal in relation to a constant reference signal. The input signal was split into two channels, which were identical except for a 90° phase

difference between them. The detectors, which operated as linear phase detectors, were each driven by equal amounts of a portion of the transmitter signal. The outputs of the detectors were

$A \sin \phi$ and $A \cos \phi$

where A is the change in signal amplitude and ϕ is the change in signal phase. It is evident that A and ϕ can be determined from the above equations.

The above circuit is basically quite simple and appeared to be well-suited to the ballistic range problem. It was in fact adopted at DRTE but was never made fully operational. A one-beam system at 70 Gc was set up. In order to obtain maximum sensitivity a superheterodyne technique was employed in which the IF was 60 mc/s and the quadrature signals were measured at 60 mc/s. It gave excellent performance and was used for many resolution experiments. However for multiple-beam operation it is complex in circuitry and in setup and operating procedures. For each beam, two IF amplifiers with precision phase characteristics are required. The LO klystron has to be phase-locked during pre-fire calibration and also during the firing. An alternative circuit which is similar in principle, but much simpler in terms of equipment and operation, has been developed at DRL and is now operational. (Ref. 11) In this, the IF is dispensed with and, instead, the signal in the wave-guide is split into two identical receiver channels. The detectors in each channel are driven by outputs from the transmitter, which are identical except that the 90° differential phase shift is inserted in one of these reference signal paths. A phase-locked oscillator is required for pre-fire calibration only. This circuit has given excellent per-formance and is believed to be one of the simplest available.

Since it was recognized from the beginning that the above circuit would require fairly extensive development work, it was decided to use circuits of lesser performance, even though it was realized that the data could not be fully interpreted. It was felt that such interim data would be extremely useful as a guide to the type of signal to be expected and might also shed some light on the ionization phenomena. One of the simplest such circuits is the one for amplitude measurements only. It has been widely used at DRTE (CARDE)[Ref. 6] and at DRL (Ref. 11). Its greatest virtue is simplicity in that only a single detector is used for each beam. The only conclusion that can be drawn from the attenuation measurement is that the amount of attenuation is due to some degree of ionization. It can be shown (Ref. 11) that attenuation is a function both of electron density and collision frequency, and they cannot be resolved separately without the use of additional information. Neverless a great deal of data has been obtained concerning radial and axial variations in ionization (see Ref. 11 and Part II of this report). An additional simple circuit which has been widely used is the one described by Whitmer, which was mentioned earlier. In this a single-channel, receiver detector is biassed with a part of the transmitter signal. The output will then be of the form A sin ϕ (the notation is the same as used in a previous paragraph) and, without additional information, A and ϕ cannot be resolved. However if it is assumed that there is no change in A (collision frequency neglected), then ϕ may be interpreted in terms of electron density. A separate amplitude measurement must be made in order to determine the collision frequency. This circuit has been used in range work (Ref. 10) but in many cases the data appeared to be meaningless, no doubt due to ambiguities.

A circuit, which is similar to the phase quadrature circuit in principle, has been developed at the RCA Victor Co, Montreal. (Ref. 14) Fixed

probes are inserted in the signal waveguide for the derivation of A sin ϕ and A cos ϕ . These two signals are fed into the X-Y amplifiers of an oscilloscope to give a polar display. The probes become an increasingly difficult proposition as the wavelength is decreased. It should also be noted that the polar coordinate display is not very suitable for range work, unless a reliable method of tracing the direction of the trace can be found, especially when several cycles of phase shift are experienced.

Phase and amplitude measuring systems have been in use at Lincoln Laboratories (Ref. 2) for several years. They appear to result in excellent performance in ballistic range work, but in general they include an IF loop and consequently they are that much more complicated than the DRL system.

THEORY OF INTERACTION OF PLANE WAVES WITH PLASMAS

To a large extent the successful application of any microwave probe to plasma diagnostics will depend on the knowledge available of the interaction of electromagnetic waves with plasmas. A considerable amount of work has been published on this subject but in a number of instances, critical problems have remained unsolved. Attention has been directed to these and to the application of other known solutions to the probe geometry.

For many purposes, the idealized case of normal incidence of a uniform, plane, electromagnetic wave on a plane, parallel-sided slab of uniform plasma is of interest. The results (reflection and transmission coefficients) are useful for order of magnitude estimates for any slab of plasma and in particular instances (focused probe for example), the results may

be directly applicable. The formal solution of this problem has, of course, been obtained and has been discussed by many authors (e.g. Ref. 15). However most of the available results were found to be in a form unsuitable for immediate use. Consequently Zivanovic (Ref. 16) has had the magnitude and phase of the transmission coefficient computed in terms of electron density collision frequency and slab length. For a given slab length, the transmission coefficient has been plotted in polar coordinates on an overlay of grids of constant electron density and collision frequency. If the slab length is known within a quarter of a wavelength, then these curves may be used to determine the electron density and collision frequency of a uniform slab from a measurement of the complex transmission coefficient. It is possible to apply this procedure to results obtained with a hypersonic wake in order to make an order of magnitude estimate of the ionization. These results will be accurate to the extent that radial gradients are absent.

It was evident (from both 35 and 70 Gc focused probe amplitude results) that strong radial ionization gradients appeared to exist in the wakes of projectiles of interest and that steps would have to be taken to determine these gradients. Two methods are being investigated. In the first method the transmission results obtained with an array of beams spaced in the radial direction are related to the electron density and collision frequency of a number of concentric uniform layers into which the wake is decomposed. The number of layers correspond to the number of beams in the array, and with a sufficient number the ionization profile can be determined with adequate accuracy. In the second method, Zivanovic (Ref. 17 and 18) has attempted to solve this problem rigorously by assuming various electron density gradients with constant collision frequency in parametric form and then computing the transmission coefficient. In the case of an exponential gradient within a

finite slab a rigorous solution was obtained (Ref. 18), but because of the higher order Bessel functions involved, which are not tabulated, and cannot yet be accurately computed in a reasonable period of time, the solution was found to be of little practical value. Instead a numerical method was developed by Zivanovic (Ref. 17) for the purpose of computing the transmission coefficient. Detailed computations have been completed for parametric forms of both exponential and parabolic distributions of electron density within a finite slab (Ref. 18). These results have been plotted in a way similar to that for a uniform slab.* By a process of trial and error the measured transmission coefficient of each beam could be matched to some particular parabolic distribution. Computing programs are now being set up by which the radial distribution may be calculated from the measured transmission of each beam according to either method. Descriptions of these programs will be given in future publications.

In the discussion of the uniform slab a rigorous treatment was assumed. This theory is cumbersome and for many purposes the underdense approximation is used. This is valid where (see Ref. 11),

$$\left| \frac{(\omega_p/\omega)^2}{1 + (\nu_c/\omega)^2} \right| << 1$$

and ω_p = plasma frequency

ω = microwave frequency

*After this work was completed, a similar method (Ref. 19) appeared in print. This latter method is a direct numerical computation of the differential equations whereas the Zivanovic method appears to be more general and flexible in that the plasma is described by matrix coefficients, which are computed. The description by matrix coefficients permits a great deal of flexibility since more complicated cases, such as composite slabs, can be treated by algebraic manipulation of the matrix coefficients (see Ref. 17).

ν_c = collision frequency

This appears to result in an excellent approximation to the transmission coefficient, and calculations are now being performed to compare it to the rigorous value for various slab parameters (see Ref. 11).

If the underdense approximation is satisfied, the complex transmission coefficient can be interpreted in terms of electron density and collision frequency in a comparatively simple way (Ref. 11). Furthermore if the plasma is assumed to be low loss i.e., $(\nu_c/\omega)^2 << 1$, then the phase of the transmission coefficient is simply proportional to the electron density and the attenuation coefficient is proportional to both collision frequency and electron density. At the present time the first of the two methods for determining the radial distribution of ionization is being programmed, based on the assumption that the transmission through each uniform layer can be interpreted according to the underdense approximation.

In all of the foregoing it has been tacitly assumed that the plasma causes no refractive effects. If these do occur, additional attenuation (analogous to deviative absorption in the theory of the ionosphere) of the transmitted energy will result, and the interpretation of the transmission coefficient by the previous methods could result in serious errors. In order to investigate refractive effects, two idealized situations have been analysed.

In the first, a uniform plane slab of plasma is located in the focal plane of a focused system (Ref. 20). The transmission coefficient is evaluated as a function of the parameters of the loss-free dielectric constant. It is found under conditions analogous to the underdense plasma

conditions, that deviative absorption can be neglected. This work is not complete and will be extended to include losses in the plasma.

In the second case, a uniform cylinder is located with its axis in the focal plane (Ref. 21). For cylinders, the diameters of which are small compared to the beam size, closed form results have been obtained. It is difficult to interpret these formulae and computations will have to be carried out. For cylinders the diameters of which are larger than the beam size, the results are similar to those above for the plane slab i.e., deviative absorption may be ignored. This work will be extended to include losses in the plasma.

There has been widespread interest shown in a resonance phenomena that had been observed experimentally. If a thin cylindrical plasma, such as is found in discharge tubes, is illuminated with microwave radiation, the polarization of which is normal to the cylinder axis, then several resonances (in reflection and transmission) occur as the discharge current is varied. Closer examination shows that the resonances are found in the region $0 \leq \frac{\omega_p}{\omega} \leq 1$. In case these might have proved troublesome in the functioning of the focused probe, and also since they might have provided a basis for a diagnostic technique, a theoretical investigation (Ref. 22) was carried out as follows.

It has been established that the anomalous resonances are due to electron acoustic waves in the cylinder. A number of important additional conclusions have been reached.

1. The wavelength of the incident radiation has to be very much greater than the diameter of the cylinder.

2. The spacing between resonances depends on the radial electron density gradients within the cylinder. If the density is uniform, the resonances are tightly bunched in the neighborhood of the main plasma resonance. If a finite gradient is assumed then the resonances are spaced much more widely apart.

3. In the analysis, the collision frequency was assumed to be zero. Although this has not been verified it is probable that these resonances will be severely damped, even in the presence of small loss.

Because of (1) and (3) it is evident that these resonances would probably not be observed in the study of hypersonic wakes with focused probes. Because of (3) it is unlikely that these resonances could form the basis of a diagnostic technique, although at extreme altitudes where the collision frequency is low, it is possible that they might be barely observable.

SECTION III. SUMMARY

It appears to be worthwhile to summarize what has been achieved by the development of the focused probe instrumentation.

1. One of the major achievements in the probe development is the confinement of the field in the neighborhood of the focus by which it has been possible to ensure tolerable diffraction errors in the measurement of transmission through wakes.
2. The field in the neighborhood of the focus is a good approximation to a plane wave which enables the interpretation of the data to be based on the idealized case of normal incidence of a uniform plane wave on a plane, parallel, plasma slab.
3. The use of several, adjacent independent beams, which is possible owing to the field confinement, described in (1), enables the radial gradients of ionization to be determined. The measurement of the complex transmission coefficient of each beam has led to an accurate, unambiguous resolution of electron density, collision frequency and their spatial gradients, without any prior knowledge of these gradients or wake sizes.
4. The use of probes at (at least) two frequencies has ensured adequate spatial resolution and a broad coverage of a range of ionization parameters.
5. The focused probe has provided the basic configuration for the focused Fabry-Perot free-space resonator. This resonator has been demonstrated to have at least two orders of magnitude improvement in sensitivity over the focused probes. It is estimated that the focused resonator could be used to measure electron densities as low as 10^9e/cc, without any loss in resolution (see Ref. 23).

PART II
APPLICATION OF FOCUSED PROBE INSTRUMENTATION TO FLOW FIELD STUDIES

The focused probe instrumentation is now virtually at the stage where detailed magnitude and spatial variations of ionization in the wakes of hypersonic projectiles can be made available on a routine basis. Some instrumentation improvements, which are mostly concerned with improving operating procedures and maintaining calibration accuracy, are now underway and are expected to be complete by the end of January 1963. The 35 and 70 Gc probes have been used to observe a large number of firings and most of this data has been processed to the stage where attenuation and phase for each beam, as a function of distance behind the body, is now available. The computer program by which the radial variation of ionization can be obtained is now being formulated and should be in operation in January 1963. The data that has been obtained will be tabulated together with comments concerning its quality and the status of data reduction. Some examples of each kind of data will be shown.

35 Gc, FOUR BEAM, AMPLITUDE DATA

Initial measurements were made with the above system. The investigations were not systematic because most of these firings were for development purposes only. Consequently they will not be tabulated. However extremely interesting phenomena were observed and two examples will be given (see also Ref. 24).

In Fig. 1, the attenuation of the axial beam is shown in relation to the projectile. Two peaks of attenuation are evident. The first is due to the interruption of the microwave beam by the projectile which cut it off almost completely. The second was postulated to be due to high electron density in the recompression zone. Later observations have confirmed this to be correct, and it is believed that this is the first reported microwave observation of the existence of the recompression zone. It is worth noting that the upper trace represents the attenuation of a beam one inch off axis. The rapid radial decay of ionization is evident. The firing conditions for Fig. 1 are given in Fig. 2d.

The existence of the so-called hollow-wake was noted in results obtained with this equipment. Examples are shown in Fig. 2. In all cases beam 3 (denoted by channel 3) intercepted the flow field along the axis. In Fig. 2a it should be noted that there is virtually no signal behind the projectile on beam 3. However, on beams 2 and 4, a small, but noticeable attenuation can be seen. One explanation of this observation is that a hollow wake forms immediately behind the body. If the pressure is held constant and the velocity is increased this phenomenom disappears and the recompression pulse can be seen again, as in Fig. 2b. These observations were repeated at different pressure and velocity conditions as shown in Figs. 2c and 2d. Careful inspection of Fig. 2d shows that the two peaks on beams 2, 3 and 4 are differently spaced. If these spacings are translated into distance and located on a shadowgraph of the model, the results shown in Fig. 3 are obtained. Here the X's indicate positions of peak attenuation on each beam. At that time, the wake shock was not visible and the lines indicating the recompression shock have been drawn through the X's. This would indicate an increase in ionization across the wake shock.

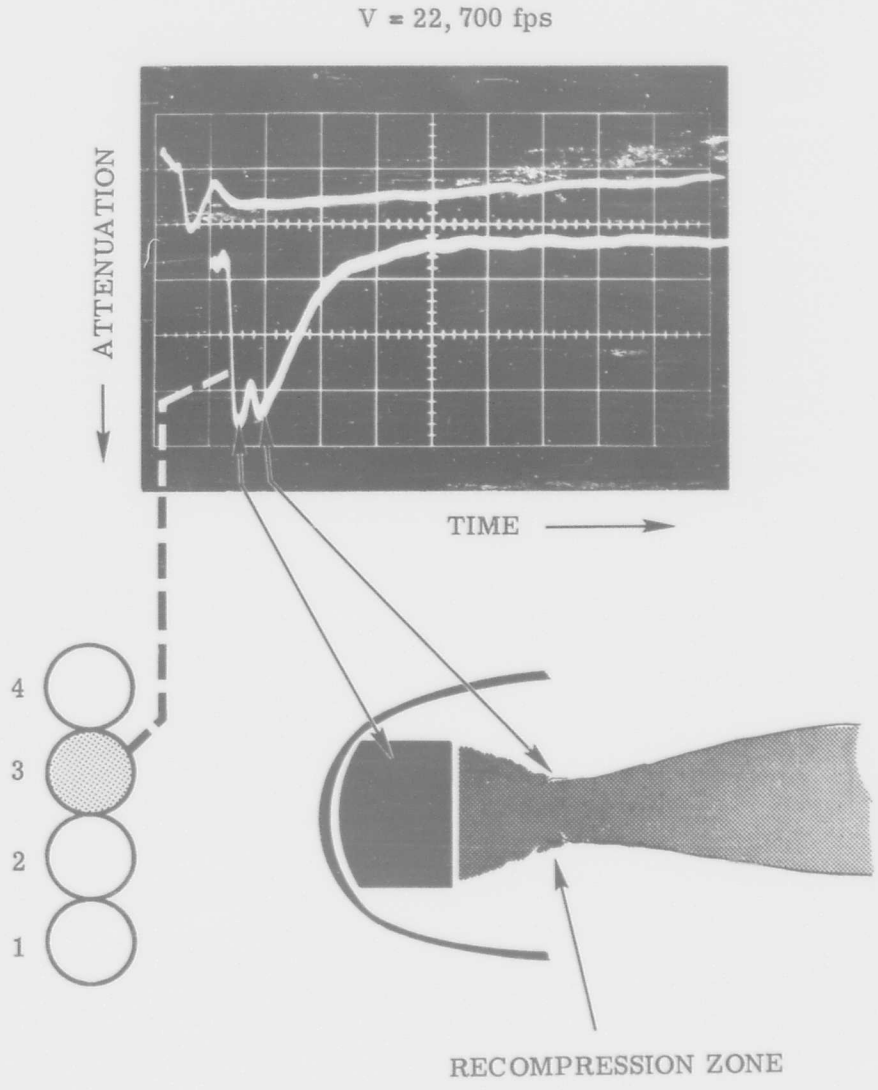

Figure 1 Attenuation of 35 Gc Beam by Hypersonic Wake

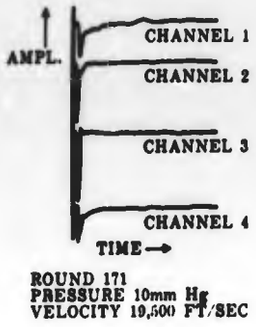

FIGURE 2a MICROWAVE PROBE DATA - ROUND 171

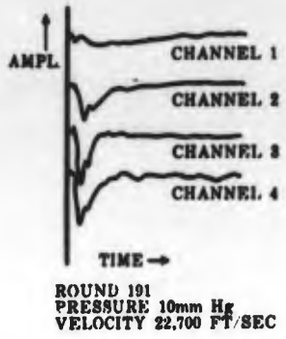

FIGURE 2b MICROWAVE PROBE DATA - ROUND 191

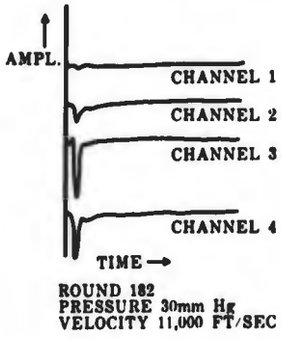

FIGURE 2c MICROWAVE PROBE DATA - ROUND 182

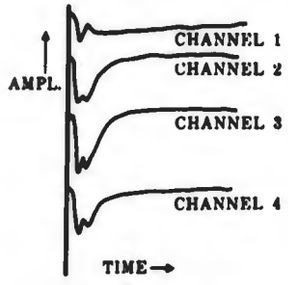

FIGURE 2d MICROWAVE PROBE DATA - ROUND 183

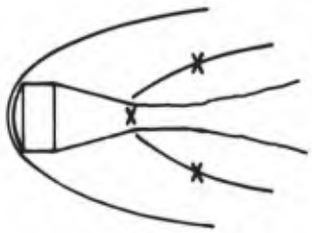

X - PULSES OCCUR ON THREE ADJACENT CHANNELS

FIGURE 3 POSITIONS OF PEAK ATTENUATION

Evidence for a hollow wake has also been obtained in two other different types of observation and will be briefly noted here.

An open shutter photograph is taken of each firing, with the camera looking down range. An example is shown in Fig. 4, in which the firing conditions are similar to those in Fig. 2a. It is evident that the wake appears to be hollow.

Image converter photographs have been taken by STL. An example is shown in Fig. 5. The appearance of what looks like a hollow wake should be noted.

In all of the firings noted above, the models were blunt-nosed cylinders made of plastic (HDPE) and undoubtedly ablated during flight. It is suggested that the hollow wake is simply due to ablation products pouring off the sides of the body into the wake.

It is planned to investigate this phenomena further by comparing the data obtained from both non-ablating spheres and ablating bodies.

70 Gc, SEVEN BEAM , AMPLITUDE DATA

This data was collected by measuring the attenuation in each beam, after passage through the wake, of a seven beam, 70 Gc system. Each beam was roughly one quarter-inch in diameter and the beams were spaced one quarter-inch apart in the plane transverse to the flight axis. Once again no systematic investigations were carried out and consequently random examples of data will be given.

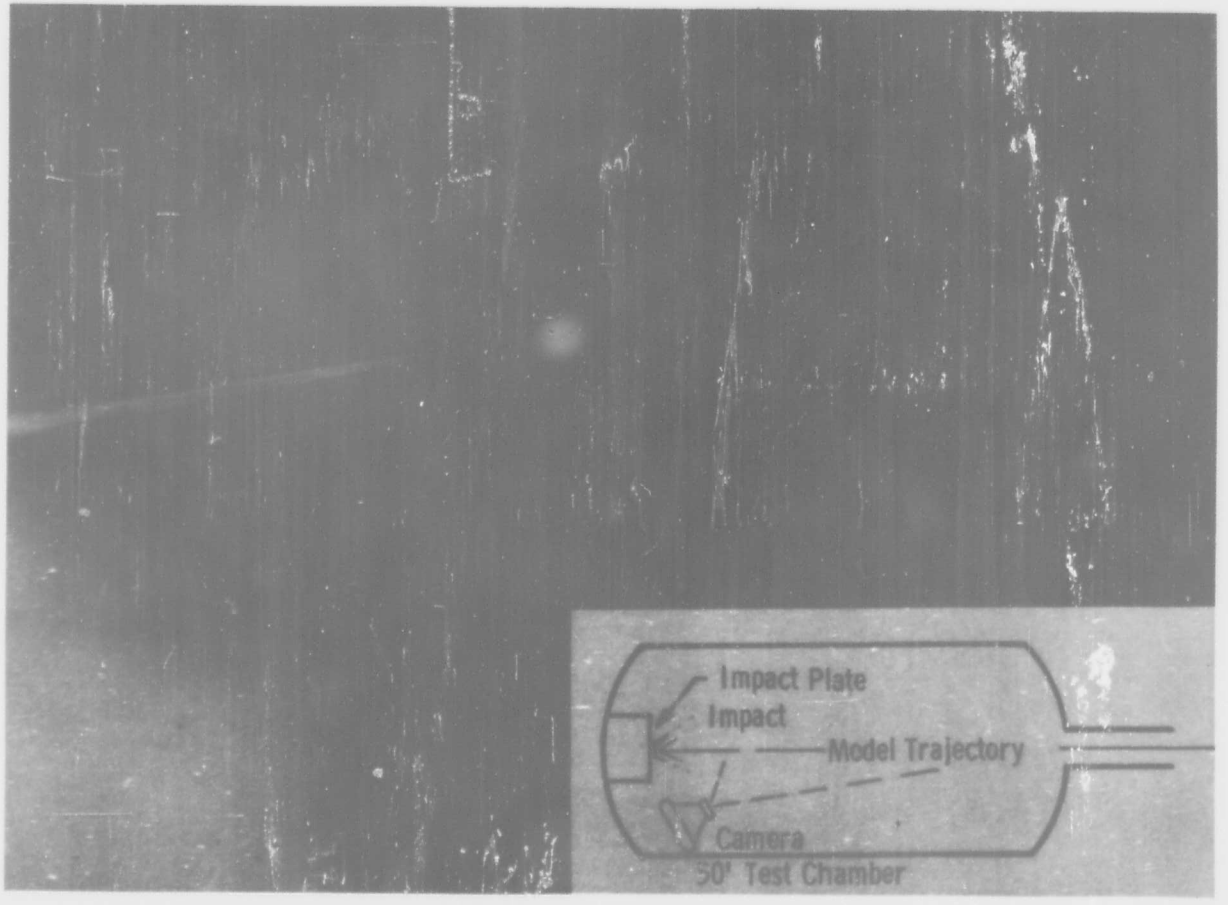

Figure 4 Open Shutter Photograph of Hypersonic Wake

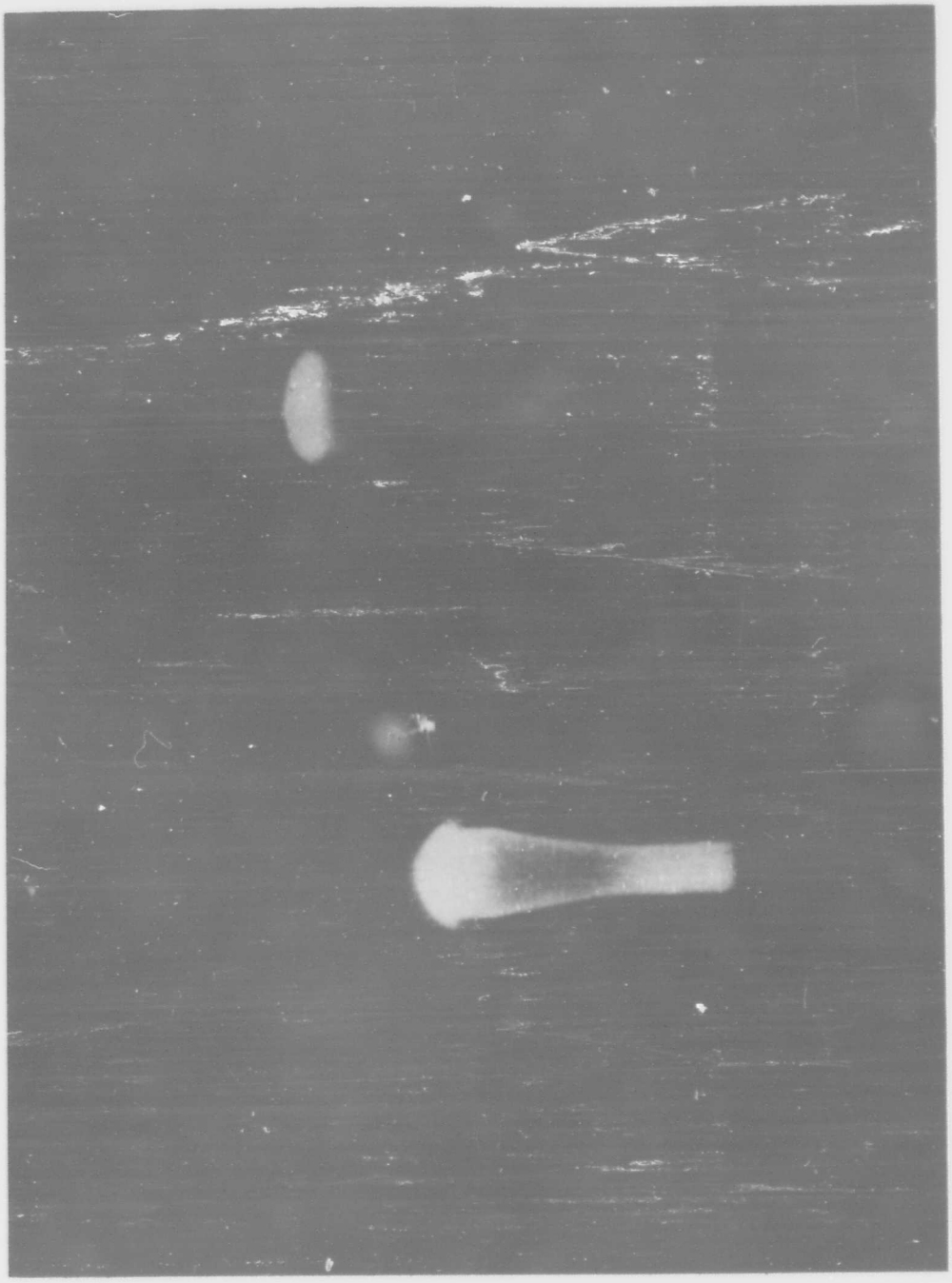

Figure 5 Image Converter Photograph of Model in Flight

It was of immediate interest to compare the resolution of this system with that of the 35 Gc probe. A typical result is shown in Fig. 6. In this case details of the flow field are visible in the shadowgraph and it can be seen that the second attenuation peak occurs very near the recompression zone. It should be noted that the recompression zone is quite clearly resolved, compared to that in the 35 Gc data (see Fig. 1).

An unexpected feature of the recompression zone, which was revealed by this data, is its minute size. In many cases it was noted that where a recompression peak is noted on the axial beam, virtually no sign of it could be seen on adjacent beams, which are only one quarter-inch off axis (see Fig. 7). Additionally it was noted that where the model had an angle of attack, the recompression zone appeared to remain on the axis of the model, rather than on the flight axis, exactly as though it were a tail attached to the body. However the transverse extent of the zone does appear to spread as a function of angle attack. These features can be seen in Fig. 8.

35 Gc, FOUR BEAM, AMPLITUDE AND PHASE DATA

This data, which is the first significant systematic data in that some meaningful interpretations can be made in terms of electron density and collision frequency, was obtained with a four-beam system. Each beam is approximately one-half inch in diameter and the beams are spaced one-half inch apart in the plane transverse to the flight direction The data has not been reduced to yield distributions, because it was felt that the four beams would not give an adequate number of data points in the radial direction. At a later stage three interlacing beams were added so that up to seven radial data points could be obtained.

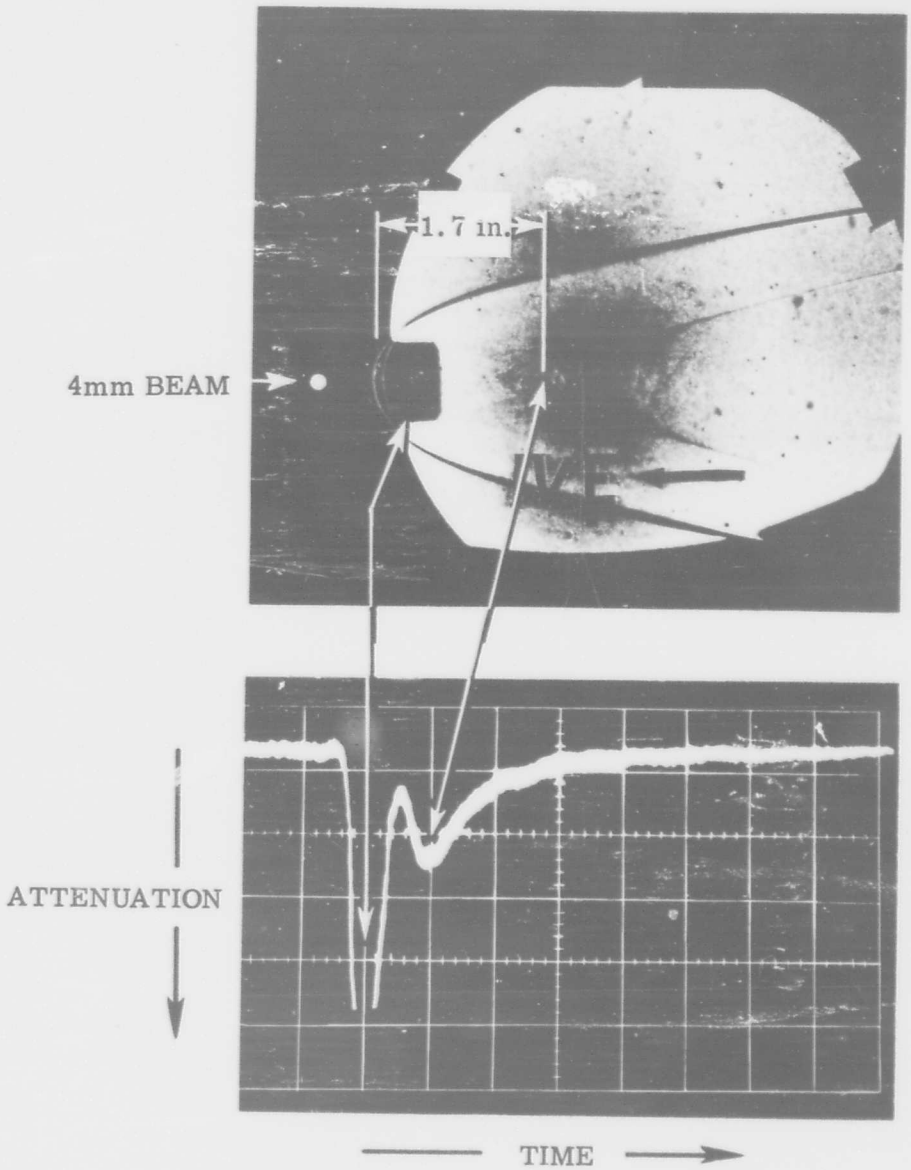

Transverse Microwave Probe:
Results with 70-Gc/s System;
V=16, 100 ft/sec, P = 106mmHg-Air

Figure 6 Attenuation of 70 Gc Beam by Hypersonic Wake

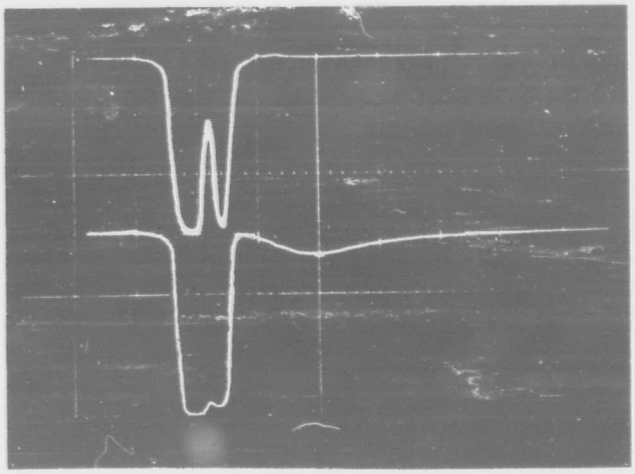

Bottom Trace: On axis
Top Trace: One quarter inch off axis
Sweep rate: 5 μsec/cm
Round 405
10 mm Hg pressure
16, 500 fps velocity

Figure 7 Attenuation of Adjacent 70 Gc Beams by Hypersonic Wake

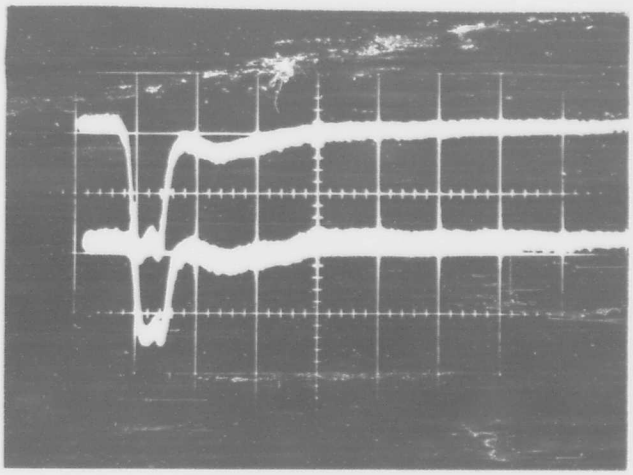

Traces are for two adjacent beams one quarter inch apart.
Sweep rate: 10 μsec/cm
Round 398
10 mm Hg pressure
14,000 fps velocity

Figure 8 Attenuation of Adjacent 70 Gc Beams by Hypersonic Wake Model with Angle of Attack

However even with the four beams it was possible to obtain a good estimate of radial ionization distributions and wake diameters.

In Fig. 9, an example is shown in which extremely strong radial gradients are evident in the near wake. In Fig. 10, an example is given of the attenuation and electron density of an axial beam. The very different decay rate (compared to Fig. 9) should be noted. A further interesting feature in Fig. 10, is that in the vicinity of the recompression zone the amplitude of the transmitted wave increases above unity. The only way that this can occur is for the dimensions of the zone to be appreciably smaller than the beam size, which is consistent with data obtained with the 70 Gc system (see Fig. 6).

A systematic study was carried out using copper-capped plastic models. The purpose was to investigate the radar absorption effect (Ref. 11) and because the velocities were low and were varied over a wide range at a fixed pressure, advantage was taken of these firings to investigate the onset of ionization and to determine the maximum useful sensitivity of the equipment. The results are shown in Figs. 11 and 12. In Fig. 11, trail length is shown as a function of velocity for two fixed pressures. At 10 mm Hg it is believed that the model was barely ablating, whilst at 100 mm Hg pressure it was most certainly ablating (it showed definite signs of breaking up at the higher velocities). The 10 mm data shows a great deal of internal consistency. The onset of ionization (at an arbitrary electron density level) is accurately defined and two sets of data taken at widely different times agree quite well. This data is plotted in a different way in Fig. 12, to show the electron density decay along the axis. Corrections have been made to allow for the variations in wake diameter as determined from the four beams. It will be noted that the data is quite consistent as a function of velocity. It

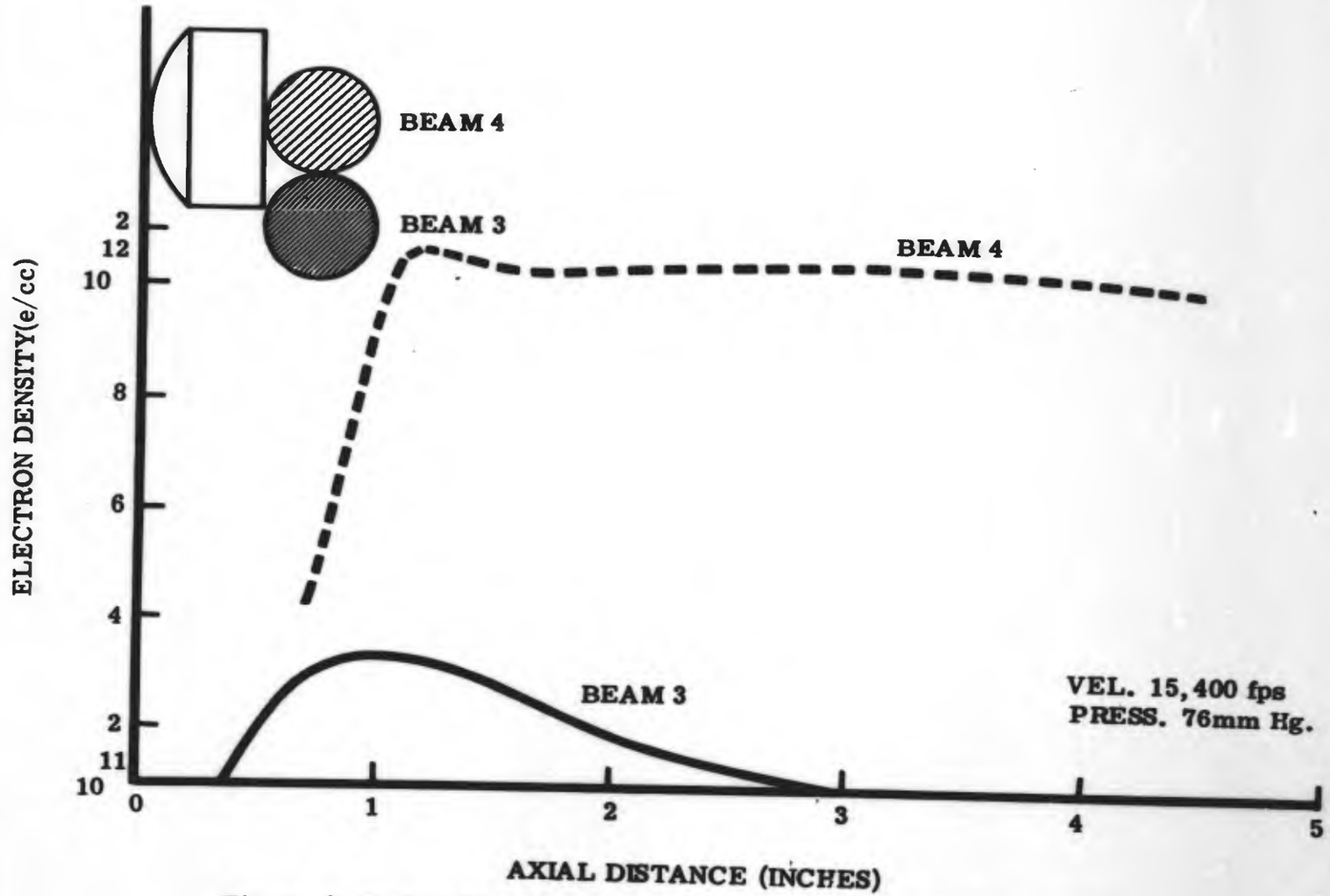

Figure 9 Radial Electron Density Gradients in Hypersonic Wake

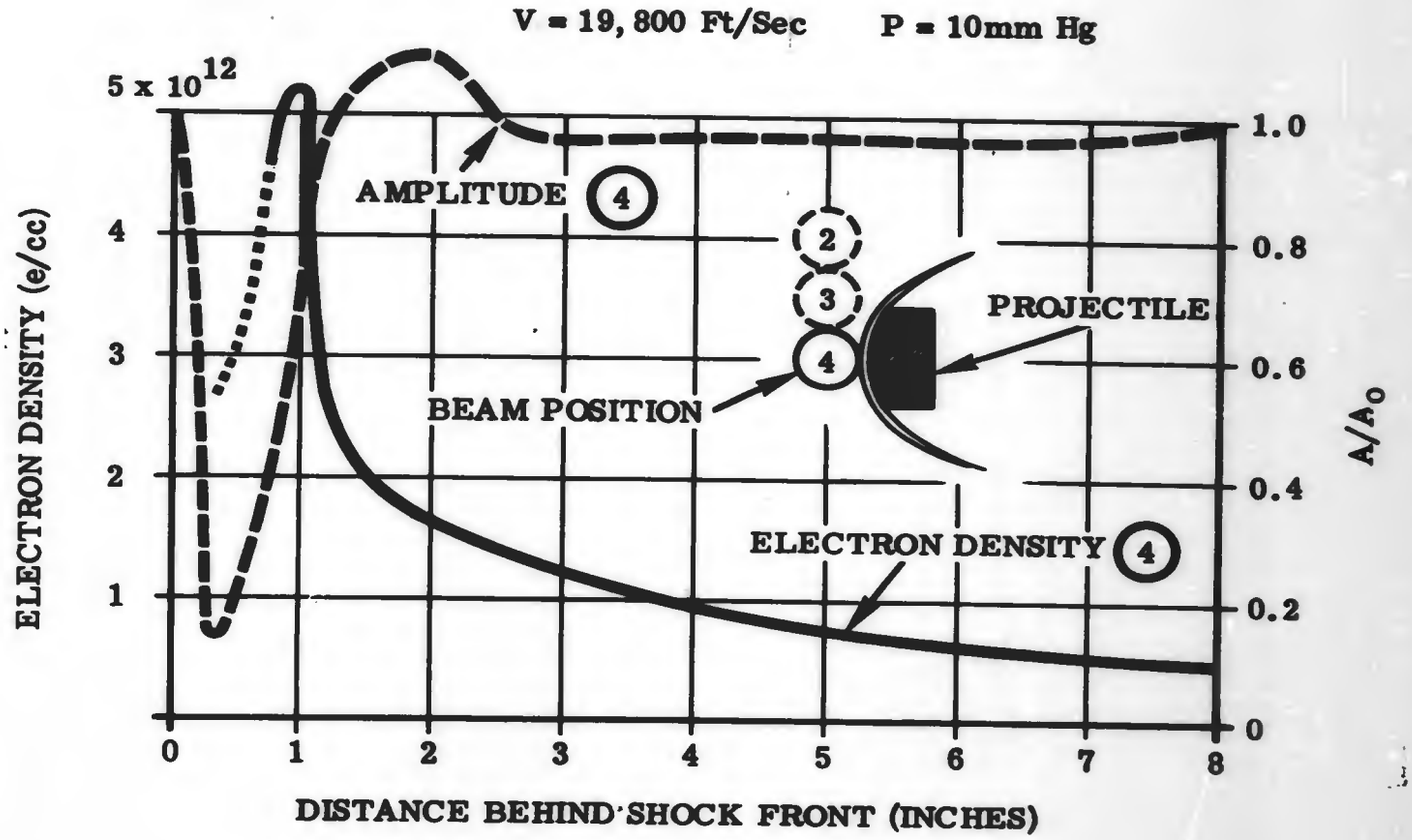

Figure 10 Attenuation and Electron Density in Hypersonic Wake

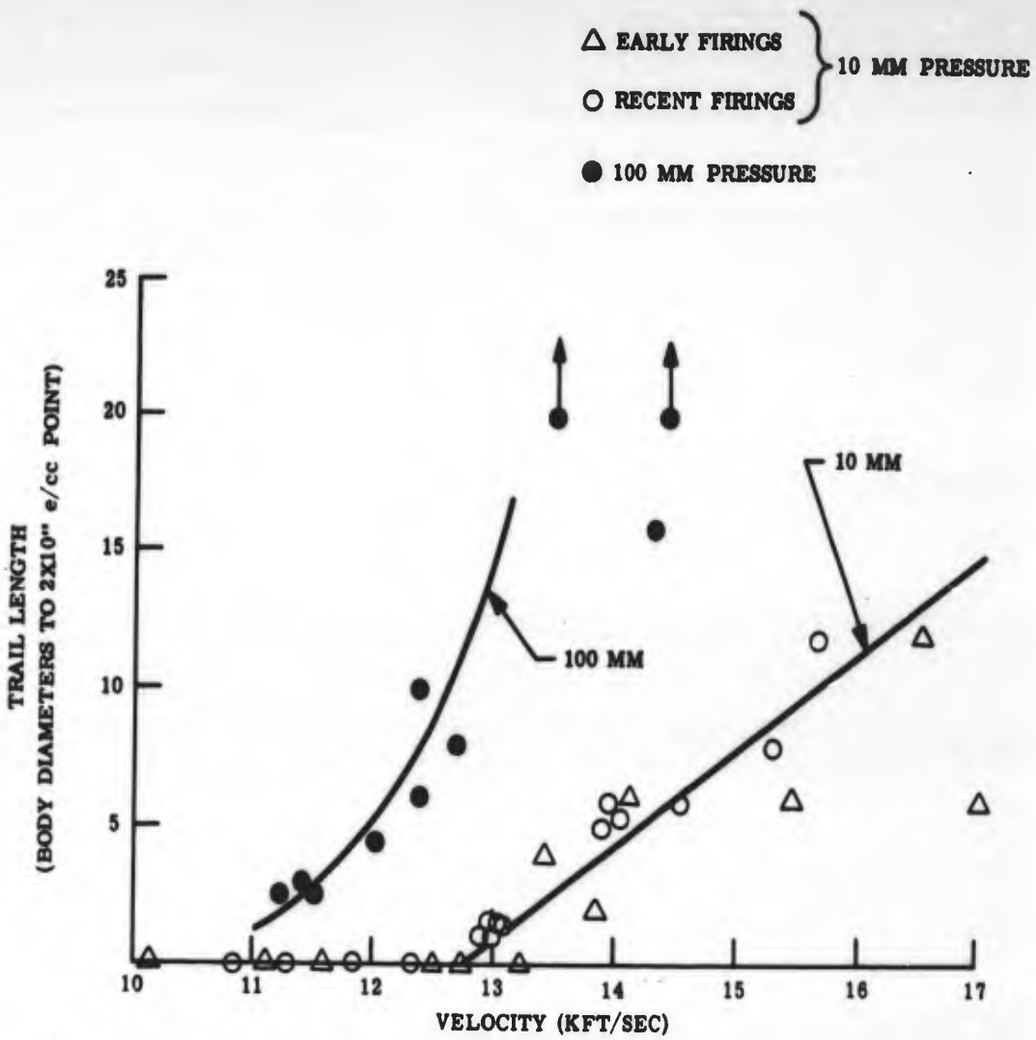

Figure 11 Onset of Ionization Behind Copper-Capped Models

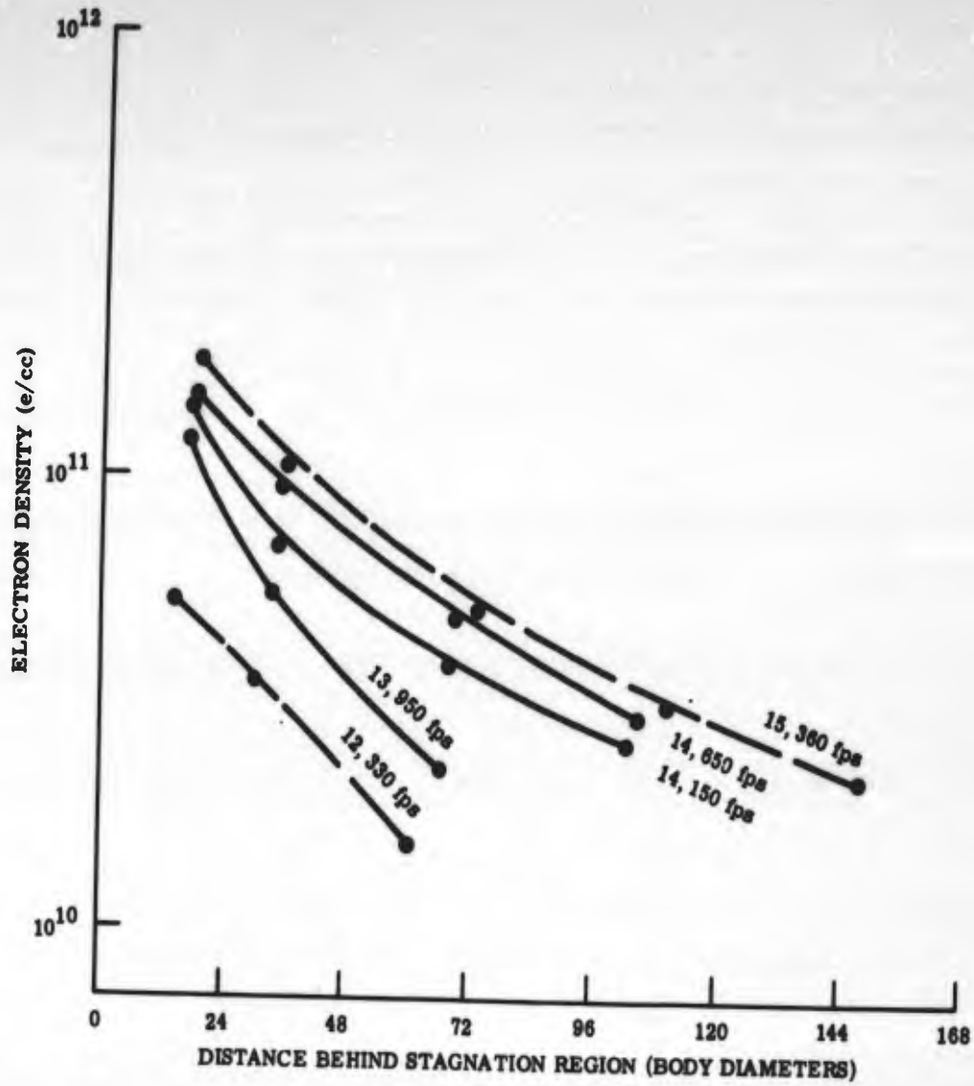

Figure 12 Electron Density Decay in Hypersonic Wakes Behind Copper-Capped Models

is also worth noting that electron densities of the order of 10^{10}e/cc can be measured consistently. A number of inconsistencies can be seen in the 100 mm data, which are undoubtedly due to uneven ablation of the model (see Fig. 11).

35 Gc and 70 Gc, SEVEN BEAM, AMPLITUDE AND PHASE DATA

Two seven-beam systems, in which the amplitude and phase shift of each beam is measured, are now fully operational. The ideal disposition of the beams in the focal plane in relation to a hypersonic wake is shown in Fig. 13. The centers of the beams in one system intersect at the same radial positions as do the beam centers in the other system.

The data obtained with the use of these probes has been tabulated in Table I. Rounds are listed in order of firing. The quality of the data and the status of the data reduction is noted alongside of each round. It will be noted that most of the data is reduced to the point where attenuation and phase per beam are available. The next step will be the reduction to yield radial and axial electron density and collision frequency gradients.

The table has been broken down further into tables which are classified according to model type as follows:

Table II	Non-ablating copper sphere. 15 mm diameter.
Table III	Copper-Capped Standard Model. Nose radius 13 mm.
Table IV	Plastic Standard Model. Nose radius 13 mm.

The rounds are listed in order of velocity for fixed pressures.

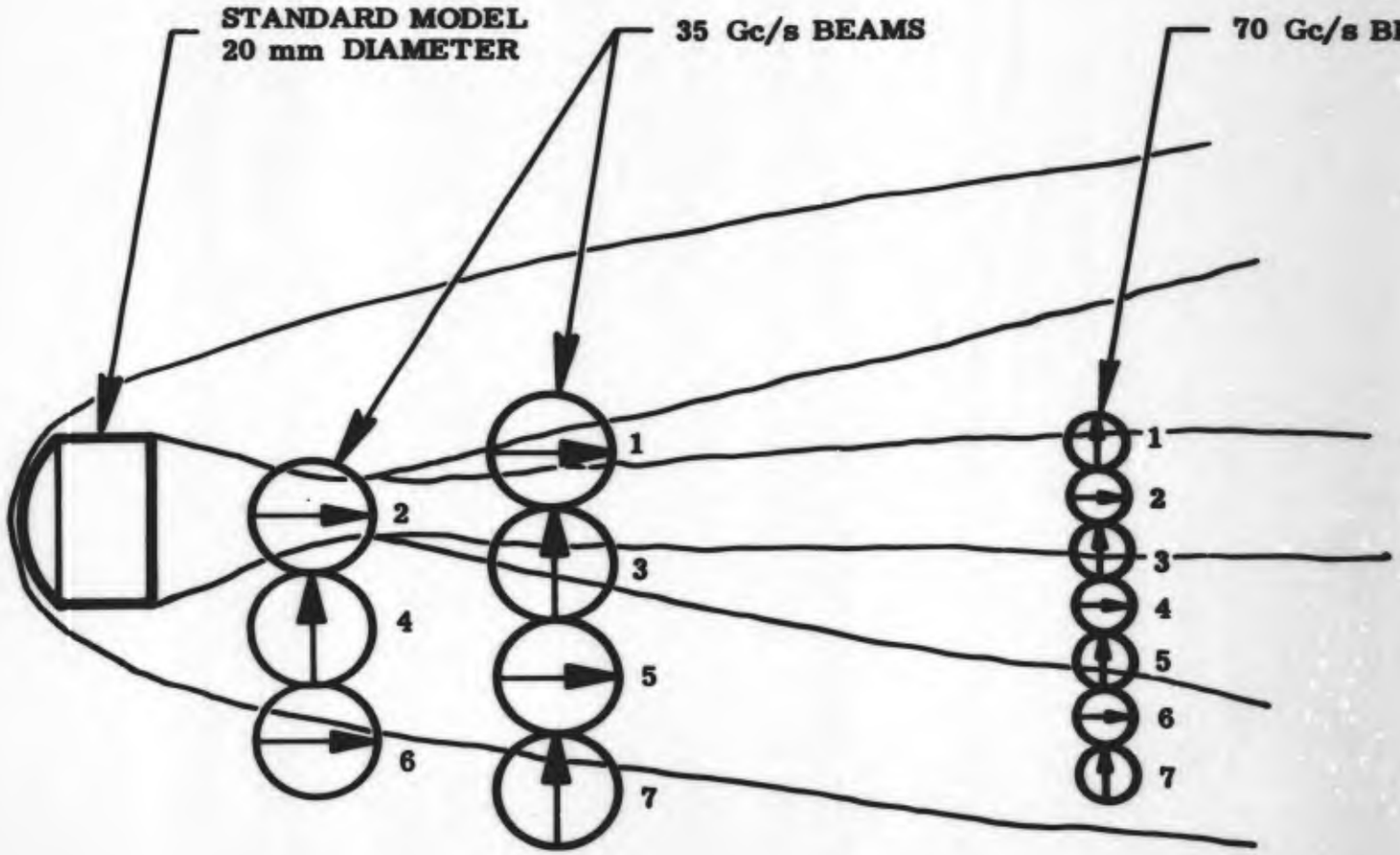

Figure 13 Ideal Disposition of Focused Beams in Hypersonic Wake

Samples of the partially reduced data will be shown to give some indication of the amount of detail revealed by the probes.

The phase and amplitude changes on each beam in a typical 70 Gc observation are shown in Fig. 14a and b. The model and flow field are shown to scale as well as the position of the model in relation to the curves and the position and sizes of the beams in relation to the model. In this special case a number of noteworthy features are self-evident. Signal peaks on adjacent channels appear at different axial positions. This is undoubtedly due to the fine beams intersecting the ionized shock front at different times. For instance there is almost a model-length delay between beam 5 (axial beam) and beam 3 which barely intercepts the model. The radial variation of ionization in the near wake is evident. An extremely interesting feature of this firing is that there appears to be definite evidence of precursor ionization (see Fig. 14b, beam 5).

Additional examples of data are given in Figs. 15a and b and Figs. 16a and b. These figures are included to indicate the agreement obtained between the two systems on a given firing.

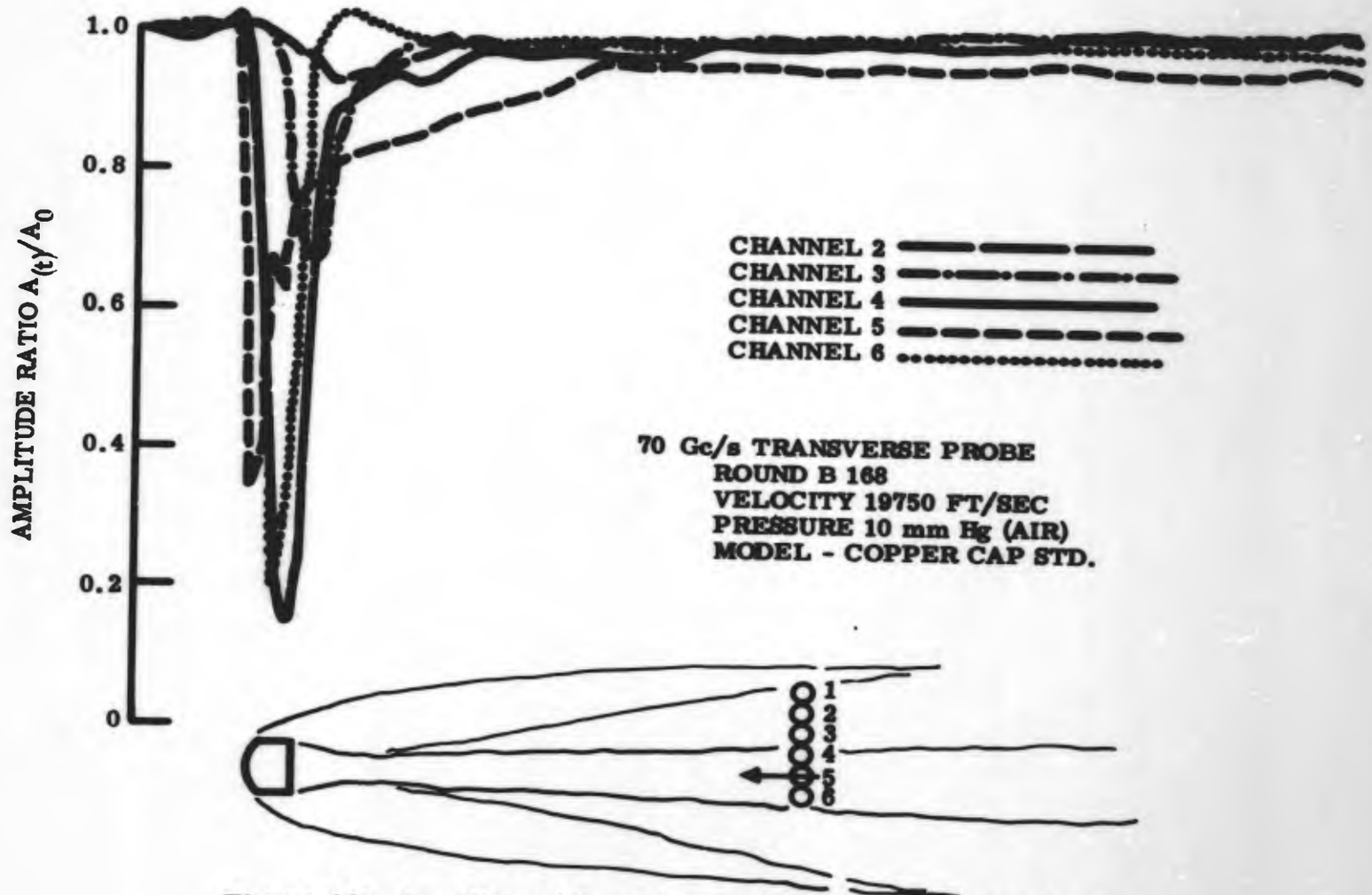

Figure 14a Amplitude Attenuation in Seven-Beam, 70 Gc System

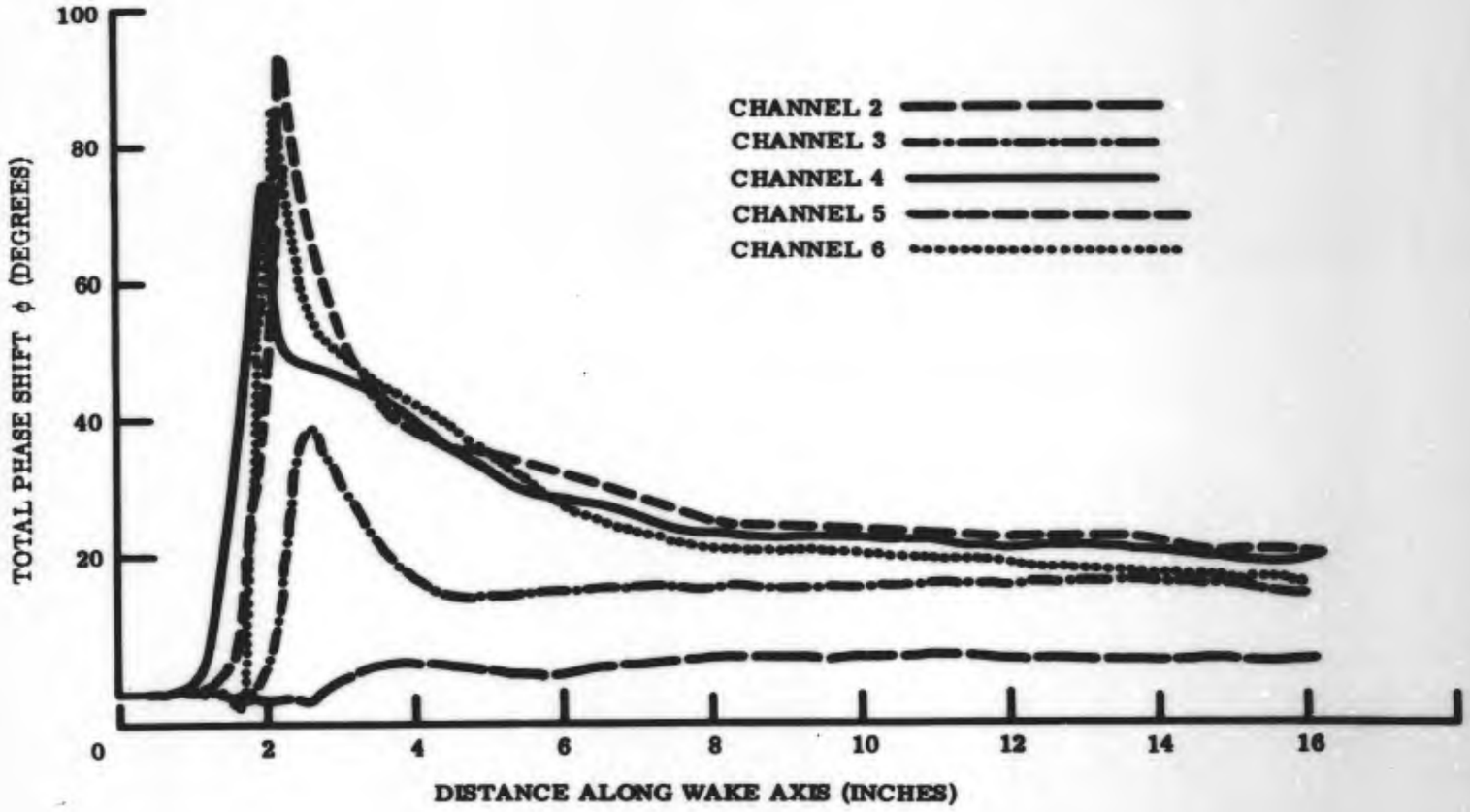

Figure 14b Phase Change in Seven-Beam, 70 Gc System

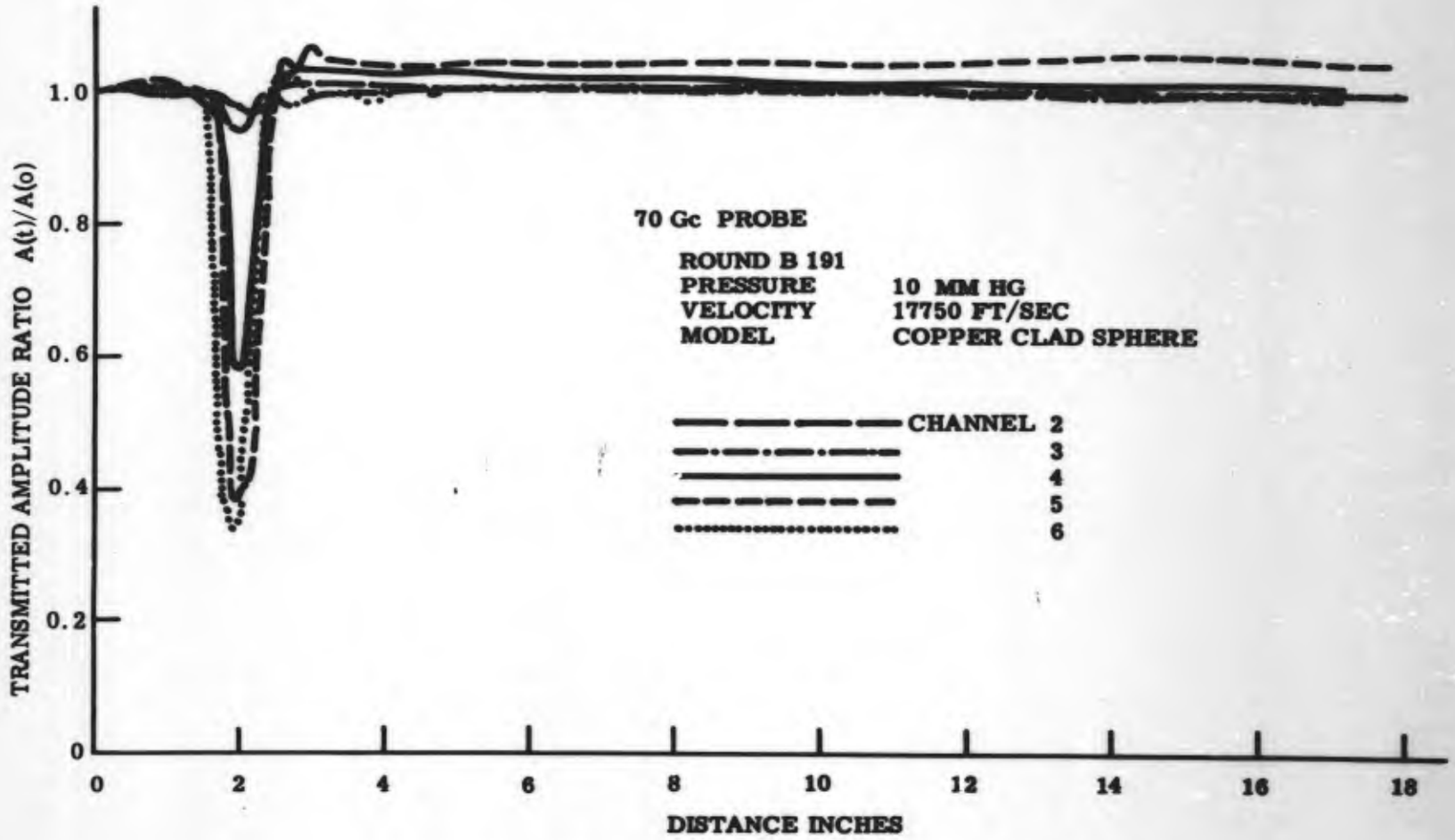

Figure 15a Attenuation in Seven-Beam, 70 Gc System

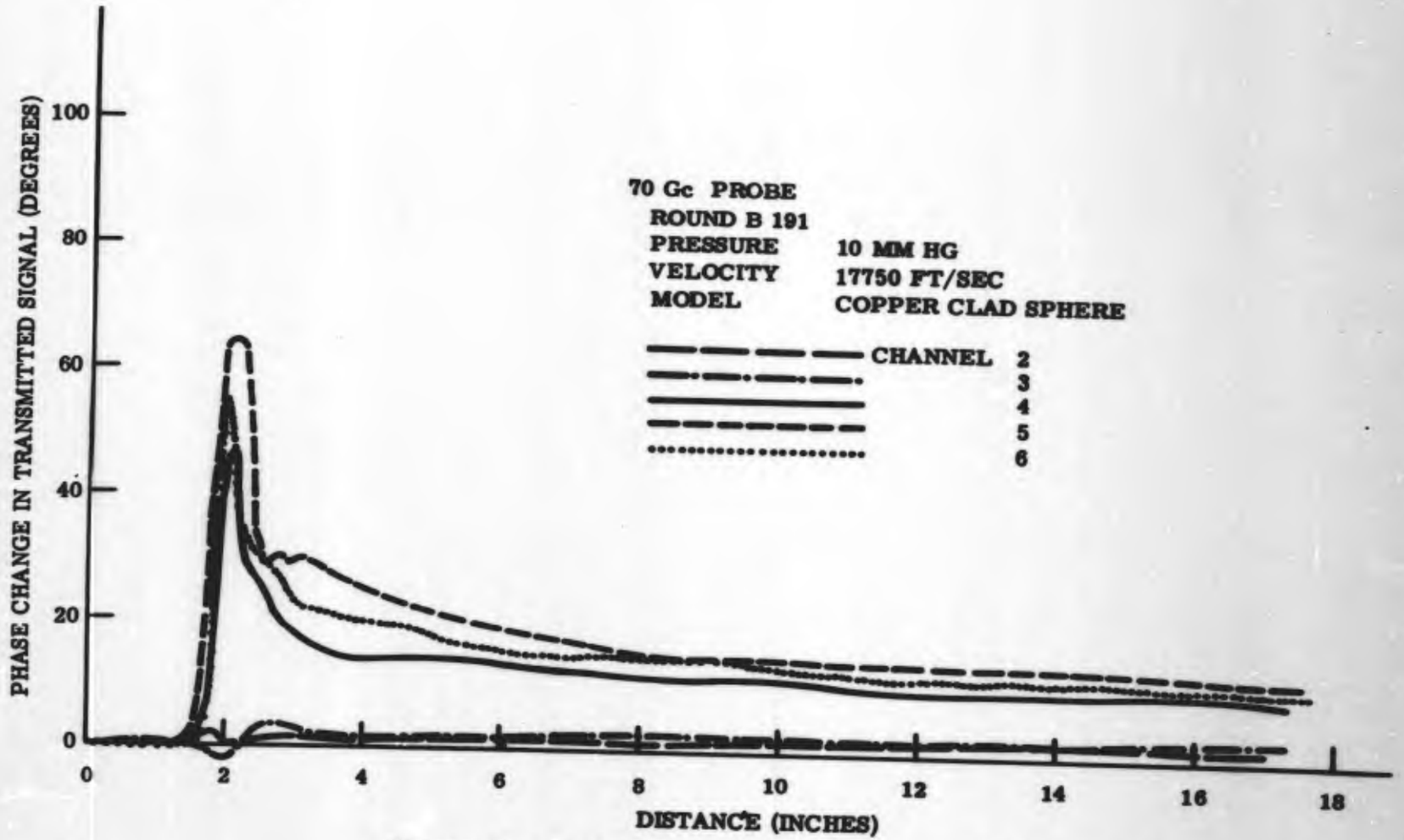

Figure 15b Phase Change in Seven-Beam, 70 Gc System

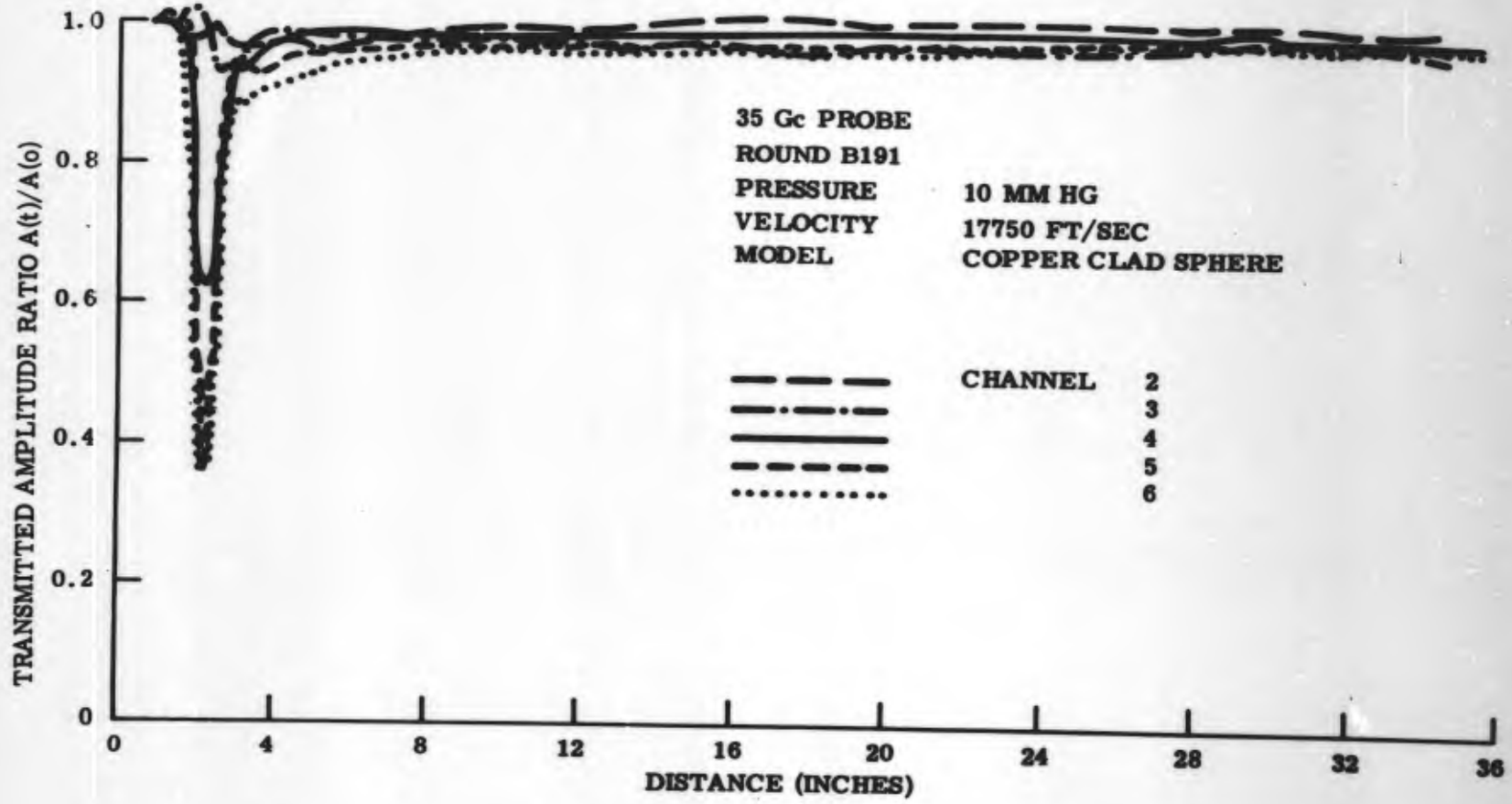

Figure 16a Attenuation in Seven-Beam, 35 Gc System

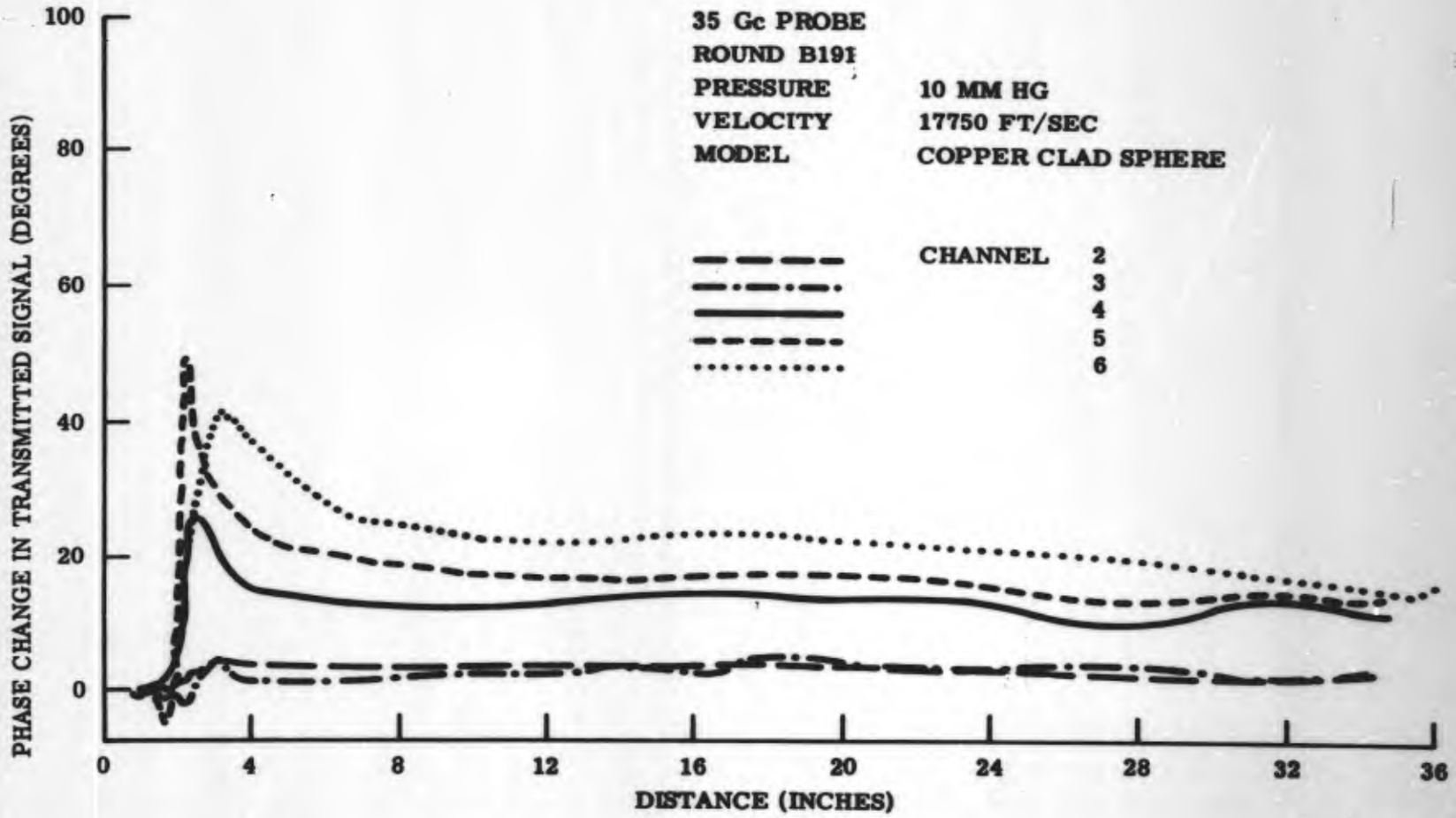

Figure 16b Phase Change in Seven-Beam, 35 Gc System

TABLE I - AIR FIRINGS - PRESSURE 10mm Hg

ROUND NO.	VELOCITY ft/sec	MODEL	35 Gc PROBE			70 Gc PROBE			REMARKS
			PHOTOS	PLOTS	COMMENTS	PHOTOS	PLOTS	COMMENTS	
B9	11,750	Cu Sphere	1 - 4	3, 4	Good	---	---	---	
B19	13,075	STD - Cu	1 - 4	2 - 4	Good	---	---	---	
B20	12,980	STD - Cu	1 - 4	3, 4	Good	---	---	---	
B22	14,050	STD - Cu	1 - 4	1 - 4	Good	---	---	---	
B23	15,300	STD - Cu	1 - 4	1 - 4	Good	---	---	---	
B24	11,300	STD - Cu	1 - 4	1 - 3	Good	---	---	---	
B25	13,900	STD - Cu	1 - 4	2 - 4	Good	---	---	---	
B26	15,650	STD - Cu	1 - 3	2, 3	Fair	---	---	---	
B46	15,300	STD - Cu	1 - 4*	2 - 4	Good	---	---	---	*Channel 3 on high gain and expanded sweep
B47	14,650	STD - Cu	1 - 3*	2, 3	Good	---	---	---	$< 15^{o}$ Tilt
B48	13,950	STD - Cu	1 - 4*	3, 4	Good	---	---	---	$< 18^{o}$
B49	11,840	STD - Cu	1 - 4*	3, 4	Good	---	---	---	$< 20^{o}$
B50	10,890	STD - Cu	1 - 4*	3, 4	Good	---	---	---	$< 5^{o}$
B51	11,490	STD - Cu	1 - 4	3, 4	Good	---	---	---	$< 10^{o}$
B52	12,330	Sphere	1, 2, 4*	4	Fair	---	---	---	$< 20^{o}$
B53	13,030	STD - Cu	1 - 4*	3, 4	Good	---	---	---	$< 10^{o}$ Tilt
B54	14,520	STD - Cu	1 - 4*	3, 4	Good	---	---	---	$< 5^{o}$

TABLE I - AIR FIRINGS - PRESSURE 10mm Hg (Continued)

ROUND NO.	VELOCITY ft/sec	MODEL	35 Gc PROBE			70 Gc PROBE			REMARKS
			PHOTOS	PLOTS	COMMENTS	PHOTOS	PLOTS	COMMENTS	
B71	12,360	STD - Cu	1 - 4*	2 - 4	Good	---	---	---	5°
B72	12,150	STD - Cu	1 - 4*	2 - 4	Good	---	---	---	
B73	12,750	STD - Cu	1 - 4*	2 - 4	Good	---	---	---	
B74	14,025	STD - Cu	1 - 4*	1 - 3	Good	---	---	---	
B75	15,360	STD - Cu	1 - 4*	2	Good	---	---	---	
B76	14,150	STD - Cu	1 - 4*	2, 3	Good	---	---	---	
B77	11,890	STD - Cu	1 - 4*	1, 2	Fair	---	---	---	Off Course
B90	13,250	STD - Cu	1,2,4*	2 - 4	Good	---	---	---	
B91	14,800	STD - Cu	1 - 4*	2 - 4	Good	---	---	---	
B92	14,675	STD - Cu	1 - 4*	1 - 4	Fair	---	---	---	< 20°
B93	13,025	STD - Cu	1 - 4*	1 - 3	Fair	---	---	---	
B95	14,140	STD - Cu	1 - 4*	1 - 4	Very Good	---	---	---	< 10°
B105	16,510	STD - Cu	1 - 4*	1 - 4	Fair	---	---	---	< 5°
B106	13,420	STD - Cu	1 - 4*	3, 4	Fair	1 - 6	1 - 4	Good	
B107	12,880	STD - Cu	1 - 4*	2 - 4	Good	1 - 6	1 - 4	Good	
B108	16,670	STD - Cu	1 - 4*	1 - 4	Good	1 - 6	1 - 6	Good	
B109	14,620	STD - Cu	1 - 4*	3, 4	Good	1 - 6	1 - 3	Good	

TABLE I - AIR FIRINGS - PRESSURE 10mm Hg (Continued)

ROUND NO.	VELOCITY ft/sec	MODEL	35 Gc PROBE			70 Gc PROBE			REMARKS
			PHOTOS	PLOTS	COMMENTS	PHOTOS	PLOTS	COMMENTS	
B113	13, 820	STD - Cu	1 - 3*	3	Fair	1 - 6	1 - 3	Good	
B114	17, 730	STD - Cu	1 - 4*	1 - 4	Good	1 - 6	1 - 6	Good	
B115	15, 550	STD - Cu	1 - 4*	3, 4	Good	1 - 6	1 - 3	Fair	
B117	11, 530	STD - Cu	1 - 4*	---	---	1 - 6	1 - 5	Good	
B121	13, 850	STD - Cu	1 - 4*	2 - 4	Fair	1 - 6	1 - 5	Good	
B123	14, 325	STD - Cu	1 - 4*	2 - 4	Good	1 - 6	1 - 6	Good	
B126	14, 450	STD - Cu	---	---	---	1 - 6	4 - 6	Poor	
B129	16, 000	STD - Cu	---	---	---	1 - 6	3 - 6	Fair	
B130	15, 100	STD - Cu	---	---	---	1 - 6	1 - 6	Fair	
B131	11, 750	Sphere	---	---	---	1 - 6	1 - 5	Poor	Break - Up
B136	10, 500	Sphere	1 - 6	1 - 6	Fair	1 - 6	3 - 6	Good	
B137	11, 500	Sphere	1 - 6	3 - 6	Poor	1 - 6	4 - 6	Good	
B138	11, 350	Sphere	1 - 6	4 - 6	Fair	1 - 6	3 - 6	Good	
B142	13, 200	Sphere	1 - 6	4 - 6	Fair	1 - 5	4, 5	Fair	
B143	13, 000	Sphere	1 - 6	1 - 6	Fair	1 - 6	3 - 6	Good	
B144	14, 090	Sphere	1 - 6	4 - 6	Fair	1 - 6	3 - 6	Good	
B145	15, 100	Sphere	1 - 6	3 - 6	Good	1 - 6	3 - 6	Good	

TABLE I - AIR FIRINGS - PRESSURE 10mm Hg (Continued)

ROUND NO.	VELOCITY ft/sec	MODEL	35 Gc PROBE			70 GC PROBE			REMARKS
			PHOTOS	PLOTS	COMMENTS	PHOTOS	PLOTS	COMMENTS	
B146	16,000	Sphere	1 - 6	1 - 6	Fair	1 - 6	1 - 6	Fair	
B147	12,650	Sphere	1 - 6	2 - 6	Good	1 - 6	3 - 6	Fair	
B148	11,330	Sphere	1 - 6	3 - 5	Good	1 - 6	3 - 5	Good	
B149	12,090	Sphere	1 - 6	---	Good	1 - 6	---	Good	Piece Trailing
B150	12,130	Sphere	1 - 6	5, 6	Fair	1 - 6	5, 6	Fair	Off Course
B151	13,750	Sphere	1 - 5	4, 5	Good	1 - 6	1 - 6	Good	
B152	17,140	Sphere	1 - 6	4 - 6	Good	1,2,3,5,6	1,5,6	Good	
B153	17,030	Sphere	1 - 6	3 - 6	Good	1 - 6	3 - 6	Good	
B155	13,260	STD - Cu	2 - 6	4 - 6	Good	1 - 6	4 - 6	Good	
B156	13,640	STD - Cu	1 - 6	3 - 6	Good	1 - 6	3 - 6	Good	
B157	15,380	STD - Cu	1 - 6	3 - 6	Good	1 - 6	4 - 6	Good	
B158	14,200	STD - Cu	1 - 6	2 - 6	Good	1 - 6	3 - 6	Good	
B159	15,920	STD - Cu	1 - 6	2 - 6	Good	1 - 6	4 - 6	Good	
B162	12,260	STD - Cu	1 - 6	4 - 6	Good	1 - 6	4 - 6	Good	
B163	15,620	STD - Cu	1 - 6	1 - 6	F - Good	1 - 6	4 - 6	Fair	
B164	12,610	Sphere	1 - 6	2 - 6	Good	1 - 6	4 - 6	Good	
B165	13,080	Sphere	1 - 6	4 - 6	Good	1 - 6	3 - 6	Good	Pieces Far Behind

TABLE I - AIR FIRINGS - PRESSURE 10 mm Hg (Continued)

ROUND NO.	VELOCITY ft/sec	MODEL	35 Gc PROBE			70 GC PROBE			REMARKS
			PHOTOS	PLOTS	COMMENTS	PHOTOS	PLOTS	COMMENTS	
B166	13,400	Sphere	1 - 6	3 - 6	Good	1 - 6	3 - 6	Good	
B167	19,450	STD - Cu	1 - 6	1 - 6	Good	1 - 6	1 - 6	Good	
B168	19,750	STD - Cu	1 - 6	1 - 6	Good	1 - 6	1 - 6	Good	
B169	22,260	STD - Cu	1 - 6	1 - 6	Fair	1 - 6	1 - 6	Good	
B171	16,150	Sphere	1 - 6	5, 6	Fair	1 - 6	5 - 6	Fair	Off Course
B172	18,460	Sphere	1 - 6	1 - 6	Good	1 - 6	3 - 6	Good	
B174	20,330	Sphere	1 - 6	1 - 6	Good	1 - 6	3 - 6	Good	
B175	11,750	STD - Cu	1 - 6	3 - 6	Good	1 - 6	3 - 6	Fair	
B176	12,170	STD - Cu	1 - 6	2 - 6	Good	1 - 6	3 - 6	Good	
B177	17,220	STD - Cu	1 - 6	1 - 6	Good	1 - 6	3 - 6	Good	
B178	11,720	STD - Cu	1 - 6	2 - 6	Good	1 - 6	3 - 6	Fair	
B179	6,660	STD - Cu	1 - 6	3 - 6	Poor	1 - 6	2 - 6	Good	
B180	12,050	STD - Y	1 - 6	3 - 6	Good	1 - 6	3 - 6	Good	
B181	12,100	STD - Y	1 - 6	2 - 6	Fair	1 - 6	2 - 6	Fair	Model Tumbled
B182	12,500	STD - Y	1 - 6	4 - 6	Fair	2 - 6	4 - 6	Good	
B183	22,040	STD - Cu	1 - 6	1 - 6	Good	1 - 6	1 - 6	Good	Elux
B184	12,530	STD - Y	1 - 6	2 - 6	F - Good	1 - 6	3 - 6	F - Good	

TABLE I - AIR FIRINGS - PRESSURE 10 mm Hg (Continued)

ROUND NO.	VELOCITY ft/sec	MODEL	35 Gc PROBE			70 GC PROBE			REMARKS
			PHOTOS	PLOTS	COMMENTS	PHOTOS	PLOTS	COMMENTS	
B185	12,630	STD - Y	1 - 6	3 - 6	Good	1 - 6	4 - 6	Good	
B186	18,000	STD - Y	1 - 6	1 - 6	Good	---	---	---	
B187	17,420	STD - Y	1 - 6	1 - 6	Good	1 - 6	1 - 6	Good	
B191	17,750	Sphere	1 - 6	2 - 6	Good	1 - 6	2 - 6	Good	
B193	16,600	STD - Cu	1 - 6	1 - 6	Good	1 - 6	1 - 6	Good	
B194	16,870	STD - Y	1 - 6	---	---	1 - 6	1 - 6	Good	
B195	17,510	STD	1 - 6	---	---	1 - 6	2 - 6	Good	HDPE
B196	17,950	STD	1 - 6	---	---	1 - 6	---	---	ZELUX
B198	19,610	Sphere	1 - 6	---	---	1 - 6	---	---	
B199	19,610	STD - Y	1 - 6	---	---	1 - 6	---	---	MODEL OSC
B200	20,810	STD - Cu	1 - 6	---	---	1 - 6	---	---	
B201	22,050	STD	1 - 6	---	---	1 - 6	---	---	HDPE
B202	19,050	STD	1 - 6	---	---	1 - 6	---	---	HDPE
B203	19,390	STD	1 - 6	---	---	1 - 6	---	---	HDPE
B204	14,710	Sphere	1 - 6	---	---	1 - 6	5, 6	---	
B205	15,970	Sphere	1 - 6	---	---	1 - 6	---	---	
B206	17,400	Sphere	1 - 6	---	---	1 - 5	---	---	

TABLE I - AIR FIRINGS - PRESSURE 10 mm Hg (Continued)

ROUND NO.	VELOCITY ft/sec	MODEL	35 Gc PROBE			70 GC PROBE			REMARKS
			PHOTOS	PLOTS	COMMENTS	PHOTOS	PLOTS	COMMENTS	
B207	21,100	Sphere	1 - 6	---	---	1 - 6	---	---	
B208	22,500	STD - Cu	1 - 6	---	---	1 - 6	---	---	
B209	22,530	STD - Cu	1 - 6	---	---	1 - 6	---	---	
B210	22,700	STD	1 - 6	---	---	1 - 6	---	---	ZELUX M
B211	22,700	STD - Cu	1 - 6	---	---	1 - 6	---	---	
B212	21,825	STD - Cu	1 - 6	---	---	1 - 6	---	---	
B213	21,800	STD - Cu	1 - 6	---	---	1 - 5	---	---	
B214	24,000	STD	1 - 6	---	---	1 - 5	---	---	HDPE
B215	23,250	STD	1 - 6	---	---	1 - 6	5, 6	---	ZELUX M
B216	23,700	STD	1 - 6	---	---	1 - 6	---	---	ZELUX M
B217	16,550	STD	1 - 6	---	---	1 - 6	---	---	ZELUX M
B218	12,490	STD	1 - 6	---	---	1 - 6	---	---	ZELUX M
B219	15,350	STD	3 - 5	---	---	---	---	---	HDPE
B221	12,350	STD - Y	1 - 6	---	---	1 - 6	---	---	
B222	16,100	STD	1 - 6	---	---	1 - 6	1 - 6	Good	ZELUX M
B231	25,950	STD	1 - 6	---	---	---	---	---	HDPE
B232	$\approx$ 26,800	STD	1 - 6	---	---	---	---	---	HDPE

TABLE I - AIR FIRINGS - PRESSURE 10 mm Hg (Continued)

ROUND NO.	VELOCITY ft/sec	MODEL	35 Gc PROBE			70 GC PROBE			REMARKS
			PHOTOS	PLOTS	COMMENTS	PHOTOS	PLOTS	COMMENTS	
B233	20,075	STD - Cu	1 - 6	---	---	1 - 6	---	---	
B234	19,800	Sphere	1 - 6	---	---	1 - 6	---	---	Pieces Trailing
B235	20,650	STD - Cu	1 - 6	---	---	1 - 6	---	---	
B236	17,500	45° Cone	1 - 6	---	---	1 - 6	---	---	Aluminum
B238	18,150	25° Cone	1 - 6	---	---	1 - 6	---	---	Aluminum
B243	17,500	90° Cone	1 - 6	---	---	1 - 6	---	---	Aluminum
B244	17,280	25° Cone	1 - 6	---	---	1 - 6	---	---	Aluminum

TABLE II - NON-ABLATING COPPER SPHERE - PRESSURE 10 mm Hg, AIR

ROUND NO.	VELOCITY ft/sec	35 Gc PROBE			70 Gc PROBE			REMARKS
		PHOTOS	PLOTS	COMMENTS	PHOTOS	PLOTS	COMMENTS	
B136	10,500	1 - 6	2 - 6	Fair	1 - 6	3 - 6	Good	
B138	11,350	1 - 6	4 - 6	Fair	1 - 6	3 - 6	Good	
B137	11,500	1 - 6	3,5,6	Poor	1 - 6	4 - 6	Good	
B9	11,750	1 - 4	2 - 4	Good	---	---	---	
B131	11,800	---	---	---	1 - 6	1 - 5	---	
B149	12,090	1 - 6	---	Good	1 - 6	---	Good	Pieces Trailing
B164	12,610	1 - 6	2 - 6	Good	1 - 6	4	Good	
B147	12,650	1 - 6	2 - 6	Fair	1 - 6	---	Fair	
B143	13,000	1 - 6	1 - 6	Fair	1 - 6	6	Good	Pieces Trailing
B165	13,080	1 - 6	4 - 6	Good	1 - 6	---	Good	Pieces Trailing
B166	13,400	1 - 6	3 - 6	Good	1 - 6	3 - 6	Good	
B151	13,750	1 - 5	4, 5	Good	1 - 6	3 - 6	---	
B144	14,090	1 - 6	4 - 6	Fair	1 - 6	3 - 6	---	
B204	14,710	1 - 6	---	---	1 - 6	---	---	Pieces Trailing
B145	15,100	1 - 6	3 - 6	Good	1 - 6	3 - 5	Good	
B205	15,970	1 - 6	---	---	1 - 6	---	---	
B146	16,000	1 - 6	1 - 6	Fair	1 - 6	1 - 6	Fair	

TABLE II - NON-ABLATING COPPER SPHERE - PRESSURE 10mm Hg, AIR (Continued)

ROUND NO.	VELOCITY ft/sec	35 Gc PROBE			70 Gc PROBE			REMARKS
		PHOTOS	PLOTS	COMMENTS	PHOTOS	PLOTS	COMMENTS	
B171	16,150	1 - 6	5, 6	Fair	1 - 6	5, 6	Fair	Off Course
B153	17,030	1 - 6	4 - 6	Good	1 - 6	4 - 6	Good	
B152	17,140	1 - 6	4 - 6	Good	1, 2, 3, 5, 6	5, 6	Good	
B206	17,400	1 - 6	---	---	1 - 5	---	---	
B191	17,750	1 - 6	2 - 6	Good	1 - 6	2 - 6	Good	
B172	18,460	1 - 6	3 - 6	Good	1 - 6	3 - 6	Good	
B173	19,500	1, 2, 4, 5, 6	1, 2, 4, 5, 6	Fair	1 - 6	1 - 6	Fair	Pieces Following
B198	19,610	1 - 6	---	---	1 - 6	---	---	
B174	20,330	1 - 6	1 - 6	Exc	1 - 6	1 - 6	Exc	
B207	21,100	1 - 6	---	---	1 - 6	---	---	

TABLE III - COPPER CAPPED STANDARD MODEL - PRESSURE 10mm Hg, AIR

ROUND NO.	VELOCITY ft/sec	35 Gc PROBE			70 Gc PROBE			REMARKS
		PHOTOS	PLOTS	COMMENTS	PHOTOS	PLOTS	COMMENTS	
B179	6,660	1 - 6	3 - 6	Poor	1 - 6	2 - 6	Good	
B50	10,890	1 - 4*	3, 4	Good	---	---	---	
B24	11,300	1 - 4	1 - 3	Good	---	---	---	
B117	11,530	1 - 4	---	---	1 - 6	1 - 5	Good	
B51	11,550	1 - 4	3, 4	Good	---	---	---	
B178	11,720	1 - 6	2 - 6	Good	1 - 6	3 - 6	Fair	
B175	11,750 ~	1 - 6	3 - 6	Good	1 - 6	3 - 6	Fair	
B49	11,840	1 - 4*	3, 4	Good	---	---	---	
B77	11,890	1 - 4*	1, 2	Fair	---	---	---	
B72	12,150	1 - 4*	2 - 4	Good	---	---	---	
B176	12,170	1 - 6	2 - 6	Good	1 - 6	3 - 6	Good	
B162	12,260	1 - 6	4 - 6	Good	1 - 6	3 - 6	Good	
B71	12,360	1 - 4*	2 - 4	Good	---	---	---	
B73	12,750	1 - 4*	2 - 4	Good	---	---	---	
B107	12,880	1 - 4*	2 - 4	Good	1 - 6	1 - 4	Good	
B20	12,980	1 - 4	3, 4	Good	---	---	---	
B53	13,030	1 - 4	3, 4	Good	---	---	---	

TABLE III - COPPER CAPPED STANDARD MODEL - PRESSURE 10mm Hg, AIR (Continued)

ROUND NO.	VELOCITY ft/sec	35 Gc PROBE			70 Gc PROBE			REMARKS
		PHOTOS	PLOTS	COMMENTS	PHOTOS	PLOTS	COMMENTS	
B19	13,075	1 - 4	2 - 4	Good	---	---	---	
B90	13,250	1 - 4	2 - 4	Good	---	---	---	
B155	13,260	1 - 6	4 - 6	Good	1 - 6	4 - 6	---	
B106	13,420	1 - 4	3, 4	Fair	1 - 6	1, 2	---	
B156	13,640	1 - 6	3 - 6	Fair	1 - 6	4 - 6	Fair	
B113	13,820	1 - 3	3	Fair	1 - 6	1, 2	Good	
B121	13,850	1 - 4	2 - 4	Fair	1 - 6	2 - 5	Good	
B25	13,900	1 - 4	2 - 4	Good .	---	---	---	
B48	13,950	1 - 4	3, 4	Good	---	---	---	
B74	14,025	1 - 4	1 - 3	Good	---	---	---	
B22	14,050	1 - 4	2 - 4	Good	---	---	---	
B95	14,140	1 - 4	1 - 4	Good	---	---	---	
B76	14,150	1 - 4	2, 3	Good	---	---	---	
B158	14,200	1 - 6	2 - 6	Good	1 - 6	3 - 6	Good	<5° Tilt
B123	14,325	1 - 4	2 - 4	Good	1 - 6	1 - 6	Good	<45° Tilt
B126	14,450	---	---	---	1 - 6	4 - 6	Poor	
B54	14,520	1 - 4	3, 4	Good	---	---	---	

TABLE III - COPPER CAPPED STANDARD MODEL - PRESSURE 10mm Hg, AIR (Continued)

ROUND NO.	VELOCITY ft/sec	35 Gc PROBE			70 Gc PROBE			REMARKS
		PHOTOS	PLOTS	COMMENTS	PHOTOS	PLOTS	COMMENTS	
B109	14,620	1 - 4	3, 4	Good	---	---	---	
B47	14,650	1 - 4	2, 3	Good	---	---	---	
B92	14,675	1 - 4	1 - 4	Fair	---	---	---	
B91	14,800	1 - 4	2 - 4	Good	---	---	---	
B23	15,300	1 - 4	1 - 4	Good	---	---	---	
B46	15,300	1 - 4	1 - 4	Good	---	---	---	
B75	15,360	1 - 4	1 - 4	Good	---	---	---	
B157	15,380	1 - 6	3 - 6	Good	1 - 6	4 - 6	Good	
B163	15,620	1 - 6	1 - 6	Good	1 - 6	4 - 6	Poor	
B26	15,650	1 - 3	2, 3	Fair	---	---	---	
B159	15,920	1 - 6	1 - 6	Good	1 - 6	4 - 6	Good	
B129	16,000	---	---	---	1 - 6	3 - 6	---	
B222	16,100	1 - 6	---	---	1 - 6	---	---	
B105	16,510	1 - 4	1 - 4	Fair	1 - 6	---	---	
B193	16,600	1 - 6	1 - 6	Good	1 - 6	1 - 6	Good	
B108	16,670	1 - 4	1 - 4	Good	1 - 6	1 - 4	Good	
B177	17,220	1 - 6	1 - 6	Good	1 - 6	3 - 6	Good	

TABLE III - COPPER CAPPED STANDARD MODEL - PRESSURE 10mm Hg, AIR (Continued)

ROUND NO.	VELOCITY ft/sec	35 Gc PROBE			70 Gc PROBE			REMARKS
		PHOTOS	PLOTS	COMMENTS	PHOTOS	PLOTS	COMMENTS	
B168	19,750	1 - 6	1 - 6	Good	1 - 6	1 - 6	Good	
B200	20,810	1 - 6	---	---	1 - 6	---	---	
B213	21,800	1 - 6	---	---	1 - 6	---	---	Elux Copper Cap
B212	21,825	1 - 6	---	---	1 - 6	---	---	
B183	22,300	1 - 6	1 - 6	Good	1 - 6	1 - 6	Good	
B211	22,700	1 - 6	---	---	1 - 6	---	---	
B209	22,800	1 - 6	---	---	1 - 6	---	---	

TABLE IV - STANDARD MODEL AIR FIRINGS - PRESSURE 10 mm Hg

ROUND NO.	VELOCITY ft/sec	MODEL	35 Gc PROBE			70 Gc PROBE			REMARKS
			PHOTOS	PLOTS	COMMENTS	PHOTOS	PLOTS	COMMENTS	
B219	15,350	STD	3 - 5	---	---	---	---	---	HDPE
B222	16,100	STD	1 - 6	---	---	1 - 6	---	---	ZELUX
B217	16,550	STD	1 - 6	---	---	1 - 6	---	---	ZELUX
B195	17,510	STD	1 - 6	---	---	1 - 6	---	---	HDPE
B196	17,950	STD	1 - 6	---	---	1 - 6	---	---	ZELUX
B202	19,050	STD	1 - 6	---	---	1 - 6	---	---	HDPE
B203	19,390	STD	1 - 6	---	---	1 - 6	---	---	HDPE
B201	22,050	STD	1 - 6	---	---	1 - 6	---	---	HDPE
B210	22,700	STD	1 - 6	---	---	1 - 6	---	---	ZELUX
B215	23,250	STD	1 - 6	---	---	1 - 6	---	---	ZELUX
B216	23,700	STD	1 - 6	---	---	1 - 6	---	---	ZELUX
B214	24,000	STD	1 - 6	---	---	1 - 5	---	---	HDPE
B231	25,950	STD	1 - 6	---	---	---	---	---	HDPE
B232	$\underset{\sim}{\wedge}$26,800	STD	1 - 6	---	---	---	---	---	HDPE
B180	12,050	STD - Y	1 - 6	3 - 6	Good	1 - 6	3 - 6	Good	
B181	12,100	STD - Y	1 - 6	2 - 6	Fair	2 - 6	4 - 6	Fair	Model Tumbled
B182	12,500	STD - Y	1 - 6	4 - 6	Fair	2 - 6	4 - 6	Good	

TABLE IV - STANDARD MODEL AIR FIRINGS - PRESSURE 10 mm Hg (Continued)

ROUND NO.	VELOCITY ft/sec	MODEL	35 Gc PROBE			70 Gc PROBE			REMARKS
			PHOTOS	PLOTS	COMMENTS	PHOTOS	PLOTS	COMMENTS	
B184	12,530	STD - Y	1 - 6	2 - 6	F - Good	1 - 6	3 - 6	F - Good	
B185	12,630	STD - Y	1 - 6	3 - 6	Good	1 - 6	4 - 6	Good	
B194	16,870	STD - Y	1 - 6	---	---	1 - 6	---	---	
B187	17,420	STD - Y	1 - 6	1 - 6	Good	1 - 6	1 - 6	Good	
B186	18,000	STD - Y	1 - 6	1 - 6	Good	---	---	---	
B199	19,610	STD - Y	1 - 6	---	---	1 - 6	---	---	

REFERENCES

1. Brown, S. C., "The Interaction of Microwaves with Gas Discharges", IRE Transactions, PGMTT-7, 1959. See also JAP. 23, pp 711, 719, 1028 (1952).

2. Lincoln Laboratories Staff. See Semiannual Technical Summary Reports on Reentry Physics Program.

3. Baldwin, K., Buck, R., Fessenden, T., & McGuire, L., "Transient Plasma Diagnostics for Wake Studies", AVCO, Research and Advanced Development Division, "Advances in Hypervelocity Techniques", Proc. Second Symposium Hypervelocity Techniques, Denver. March 1962.

4. Schoonaver, M., Siperly, B., and Short, W., "Microwave Studies of Flow Fields around Hypervelocity Projectiles", General Dynamics/Astronautics, Physics Section ZPh-094, 30 June 1961, Contract DA-04-495-ORD-3112, p. 19.

5. Recent measurements at General Motors Defense Research Laboratories, Santa Barbara.

6. Primich, R. I., "Microwave Techniques for Hypersonic Ballistic Ranges", Electromagnetic Effects of Re-entry, Pergamon Press, 1961, pp 186-195.

7. See, for instance, NRL Rpt. 4669 and bibliography therein.

8. Dagai, M., "Techniques et Equipements de Mesure de Densite de Plasma de L'ordre de $10^{14}e/cm^3$," Ionization Phenomena in Gases, Conference in Munich, 1961.

9. Lashinsky, H., Private Communication.

10. Hayami, R. A., "A Microwave Interferometer Using High Resolution Focused Beams for Plasma Studies", Paper presented at IRE Conference, Toronto, Canada, October, 1961.

11. Instrumentation, Calibration Methods and Data Reduction Methods, General Motors Defense Research Laboratories, TR62-213, December, 1962.

12. Primich, R. I., and Northover, F. H., Use of Focused Antenna for Ionized Trail Measurements, DRTE Rpt. 1076, October 1961, Defense Research Telecommunications Establishment, Shirley Bay, Ottawa, Canada. (Also to be published in IRE Transactions, PGAP, March 1963.)

13. Whitmer, R. F., "Microwave Studies of the Electron Loss Processes in Gaseous Discharges", Phys. Rev., 104 (1956), p. 572.

14. Bachynski, M. P., Private Communication.

15. Budden, K. G., Radio Waves in the Ionosphere, Cambridge Univ. Press, 1961.

16. Zivanovic, S., "Transmission and Reflection Coefficients of Uniform Plasma Slabs as a Function of Electron Density, Collision Frequency and Thickness", General Motors Defense Research Laboratories, TR62-209 I.

17. Zivanovic, S., "A Numerical Method for the Determination of Transmission and Reflection Coefficients of a One Dimensional Plasma Slab", General Motors Defense Research Laboratories, TR62-209J.

18. Zivanovic, S., "Transmission and Reflection Coefficients of a One Dimensional Plasma Slab with Parabolic Electron Density Distribution", General Motors Defense Research Laboratories, TR62-209K.

19. Nicoll, G. R., and Basu, J., "Reflection and Transmission of an Electromagnetic Wave by a Gaseous Plasma", Proc. I.E.E. (London), Part C., p. 335, 1962.

20. Northover, F. H., "The Incidence of Focused Microwaves upon Ionized Distributions", Part I. Plane Distributions, General Motors Defense Research Laboratories, TR62-209N.

21. Northover, F. H., "The Incidence of Focused Microwaves upon Ionized Distributions," Part II. Cylindrical Distributions, General Motors Defense Research Laboratories, TR62-209O.

22. Fejer, J. A., "Scattering of Electromagnetic Waves by a Plasma Cylinder", General Motors Defense Research Laboratories, TR62-209L.

23. Primich, R. I., and Hayami, R. A., "Millimeter Wavelength Focused Probes and Focused Resonant Probes for Studying the Ionized Wakes Behind Projectiles in Free-Flight Ranges", Paper to be given at Millimeter Conference, Orlando, Florida, January 1963.

24. Primich, R. I., Hansen, C. F., and Charters, A. C., "Measurements of Re-entry Radar Characteristics in Free-Flight Range", 12th AMRAC Meeting, Santa Barbara, November 16, 1961.

DISTRIBUTION

Recipient	Copy No.
Commander, U.S. Army Missile Command Redstone Arsenal, Alabama ATTN: ORDXM-RRX	1-12
Advanced Research Projects Agency The Pentagon Washington 25, D.C. ATTN: Lt. Col. Cooper Ballistic Missile Defense Office	13,14
Aerojet-General Corporation Azusa, California ATTN: C. Dunning	15
Aeronutronic Division Ford Motor Company 1234 Air Way Glendale, California ATTN: Dr. John Hall	16
Aerospace Corporation P.O. Box 4007 Patrick AFB, Florida ATTN: Dr. Martin Gould Classified Documents Control	17
Aerospace Corporation Classified Information Control 2400 E. El Segundo Blvd El Segundo, California ATTN: Dr. D. Bitondo	18
Aerospace Technical Intelligence Center U.S. Air Force Wright-Patterson Air Force Base, Ohio ATTN: AFCIN-4F3B	19
Air Force Ballistic Missile Division BSRUT AF Unit Post Office Los Angeles 45, California ATTN: Major William W. Levy	20
Air Force Command and Control Dev. Div. Air Research and Development Command L.G. Hanscom Field Bedford, Massachusetts ATTN: CCO-Range Measurements Office	21
Headquarters ARDC Andrews Air Force Base Washington 25, D.C. ATTN: RDRC	22
Armed Services Tech. Infor. Agency Arlington Hall Station Arlington 12, Virginia ATTN: J. Heaton Heald	23-32
Research and Advanced Dev. Div. Avco Corporation Wilmington, Massachusetts ATTN: H.S. Flickinger Chief, Data Evaluation and Analysis	33
Avco-Everett Research Laboratory 2385 Revere Beach Parkway Everett, Massachusetts	34
Ballistics Research Laboratories Exterior Ballistics Laboratory Aberdeen, Maryland ATTN: Dr. C. Murphy	35
Barnes Engineering Company 30 Commerce Road Stamford, Connecticut	36
Batelle Memorial Institute 505 King Avenue Columbus 1, Ohio ATTN: Battelle-Defender	37
Bell Telephone Laboratories, Inc. Whippany, New Jersey ATTN: Mr. C.W. Hoover, Rm 2B-105	38
The Bendix Corporation Bendix Systems Division 3300 Plymouth Road Ann Arbor, Michigan ATTN: Systems Analysis and Mathematics Dept.	39
Commanding Officer Bureau of Naval Weapons Washington, D.C. ATTN: FASE, Dept. of the Navy	40

Recipient	Copy No.
Chief, Bureau of Naval Weapons Navy Department Washington 25, D. C. ATTN: RMWC-322	41
Brown Engineering Company Custodian, Central Security Files P. O. Drawer 917 Huntsville, Alabama ATTN: H. Crews	42
Cornell Aeronautical Laboratory, Inc. 4455 Genesee Street Buffalo 21, N. Y. ATTN: J. Lotsof W. Wurster	43, 44
Electro-Optical Systems, Inc. 125 N. Vinedo Avenue Pasadena, California ATTN: Mr. Denison	45
General Dynamics/Astronautics San Diego, California ATTN: Mr. K. G. Blair Chief Librarian Mail Zone 6-157 for W. Hooker 6-172	46
General Electric Company - MSVD Space Sciences Laboratory 3750 D Street Philadelphia, Pa. ATTN: Re-Entry Physics Library	47
Technical Information Center General Electric Company, MSVD Room 3446, 3198 Chestnut Street Philadelphia 4, Pa. ATTN: Mr. Lawrence I. Chasen Manager, Tech Info Center	48
Geophysics Corporation of America Burlington Road Bedford, Massachusetts ATTN: John W. Bond, Jr.	49
Heliodyne Corporation 2365 Westwood Blvd. Los Angeles, California	50
Jet Propulsion Laboratory 4800 Oak Grove Drive Pasadena, California ATTN: Hunston Denslow Library Supervisor	51
Applied Physics Laboratory The John Hopkins University 8621 Georgia Avenue Silver Spring, Maryland ATTN: Mr. George L. Seielstad	52
Kaman Nuclear Division Colorado Springs, Colorado ATTN: Dr. A. P. Bridges	53
Instrument Research Division Langley Research Center Langley Field, Virginia ATTN: Howard B. Edwards	54
Lincoln Laboratory, MIT P. O. Box 73 Lexington 73, Massachusetts ATTN: Library, D-224 G. Pippert	55
Lockheed Missiles and Space Division Sunnyvale, California ATTN: Ray Munson	56
Melpar Inc. Applied Science Division 11 Galen Street Watertown 72, Massachusetts ATTN: M. J. Cryer	57
The MITRE Corporation Bedford, Massachusetts ATTN: Supervisor Library Services	58
Office of the Director Technical Analysis and Advisory Group (OP-07T3E) Deputy Chief of Naval Operations (Development) The Pentagon Washington 25, D. C.	59
Chief of Naval Operations Navy Department Washington 25, D. C. ATTN: OP732	60
Chief of Ordnance Hdqt. Dept. of the Army Washington 25, D. C. ATTN: ORDTU	61

Recipient	Copy No.
RAND Corporation 1700 Main Street Santa Monica, California ATTN: Library (M. H. Davis)	62
Raytheon Company Missile Systems Division Bedford Res. and Dev. Center Bedford, Massachusetts ATTN: Mrs. I. Britton, Librarian	63
Stanford Research Institute Documents Center Menlo Park, California ATTN: Acquisitions	64
Space Technology Laboratories P. O. Box 95001 Los Angeles 45, California ATTN: Mr. L. McFadden	65
Space Technology Laboratories Titan Program Director P. O. Box 95001 Los Angeles, California ATTN: A. C. Anchordough	66
Special Projects Office Department of the Navy Washington 25, D. C. ATTN: SP-2721	67
The Radiation Laboratory Department of Electrical Eng. University of Michigan 201 E. Catherine Ann Arbor, Michigan ATTN: Dr. Richard J. Leite	68
University of Michigan Willow Run Laboratories Technical Document Service P. O. Box 2008 Ann Arbor, Michigan ATTN: Bamirac Library/B. R. George	69
Command and Control Systems Division Directorate of Systems Development Headquarters, Room 4D324 The Pentagon Washington 25, D. C. ATTN: Major R. J. Kaminski U. S. Air Force	70
Commanding General U. S. Army Air Defense Command Ent Air Force Base Colorado Springs, Colorado ATTN: Advanced Projects Division, G-3	71
Commander U. S. Army Ordnance Missile Command Redstone Arsenal, Alabama ATTN: Technical Library	72
U. S. Army Liaison Office Canadian Armament Res and Dev Establishment P. O. Box 1427 Quebec, P. Q., Canada ATTN: Lt. Col. E. W. Kreischer	73
Director U. S. Naval Research Laboratory Washington 25, D. C. ATTN: Code 2027	74
Director Weapons Systems Evaluation Group Pentagon, Room 1 E 800 Washington 25, D. C.	75
Defense Research Laboratories	76 and above

UNCLASSIFIED